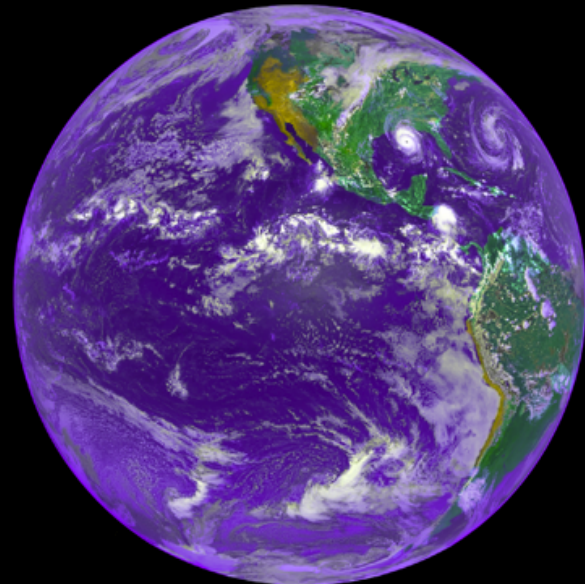


# Radial basis functions: A mesh-free modeling framework for computational geosciences



Grady B. Wright  
Boise State University

\*This work is supported by NSF CMG grant DMS 0934581

In case you didn't know...

---

Geo Seminar,  
Oct. 21, 2013

# Mathematics of Planet Earth

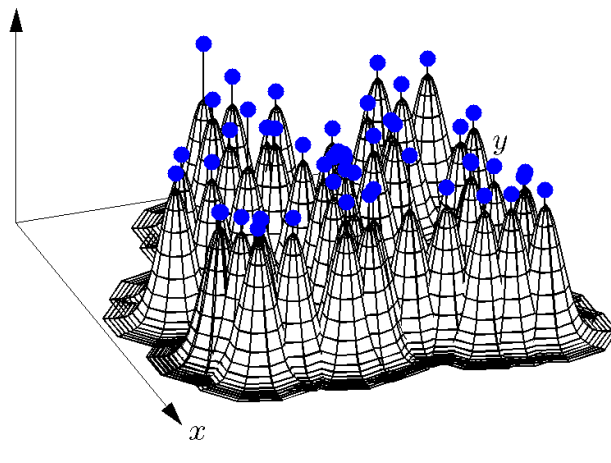


2013

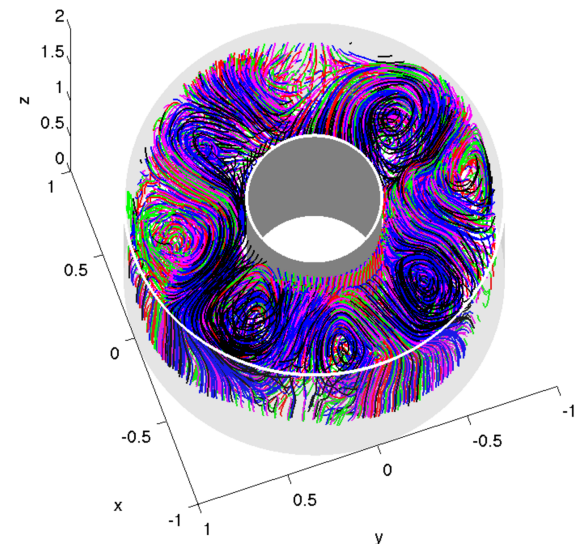


# Overview

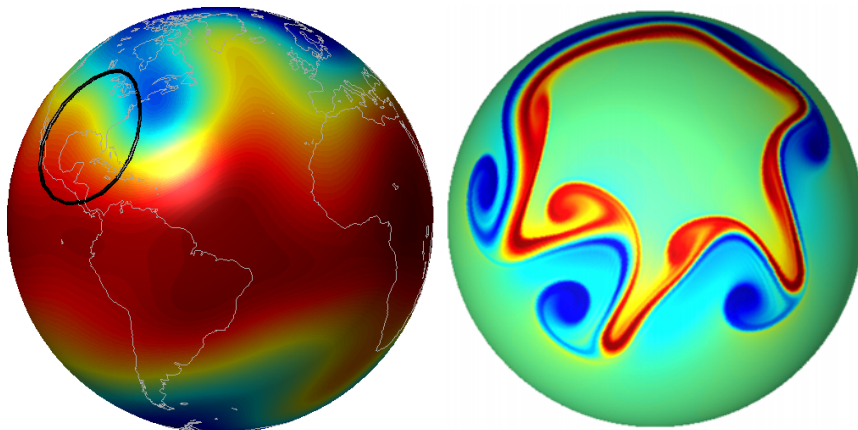
Overview of radial basis function  
interpolation



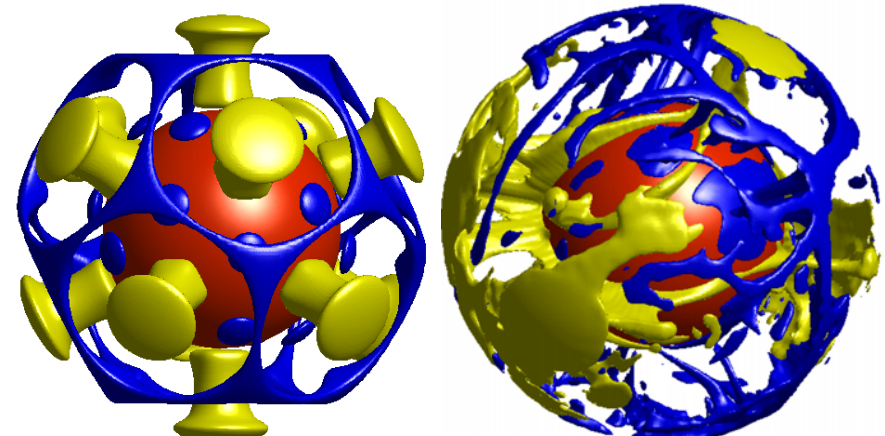
Differentially heated rotating annulus:  
Baroclinic instability



Shallow water flows:  
numerical weather prediction

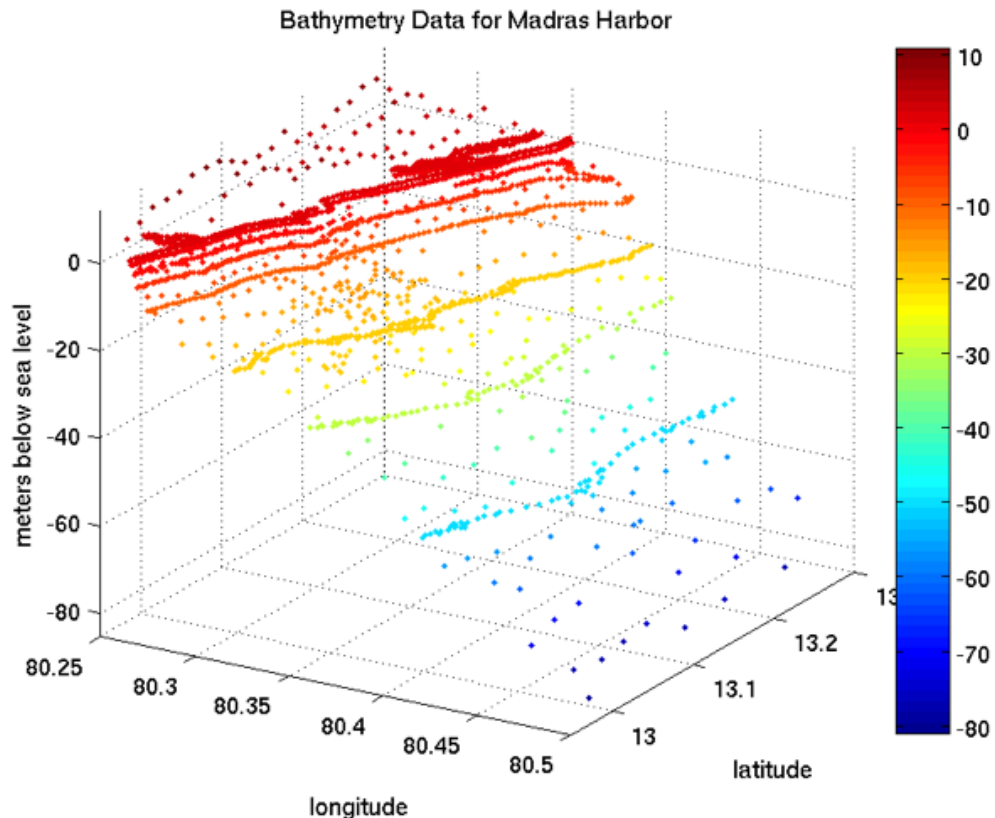


Rayleigh-Bénard Convection:  
Mantle convection



# Scattered data approximation

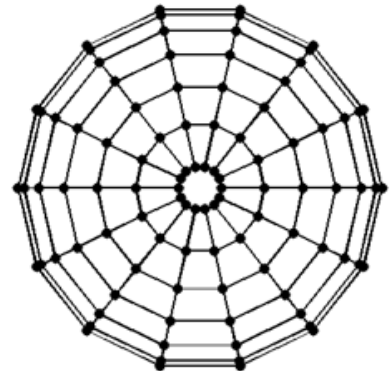
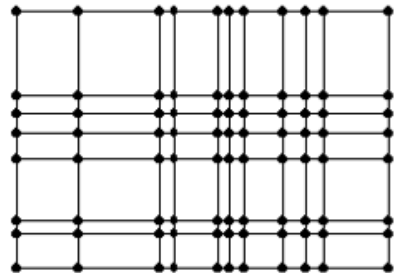
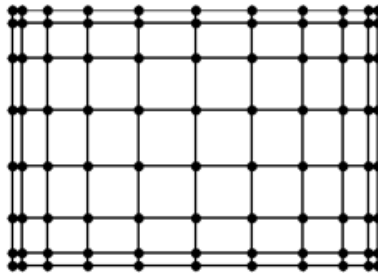
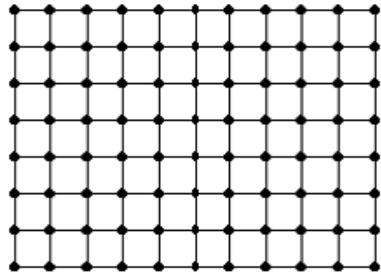
- Problem: construct a continuous surface that approximates a given set of data.



- Non-trivial to generalize standard methods for this task in 1D to higher dimensions.

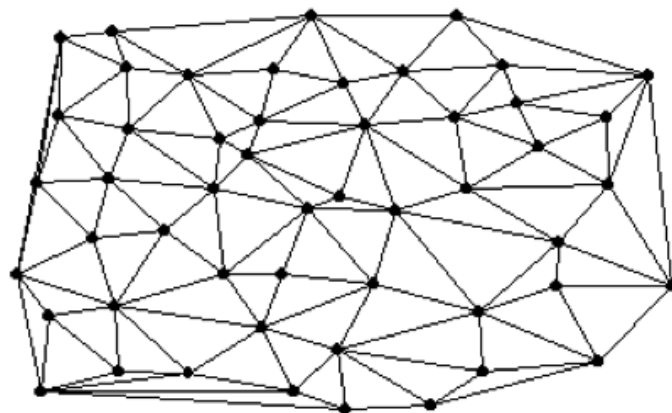
# Grid and mesh-based methods

- Tensor product grids:



Methods: Polynomials, Fourier, splines, etc.

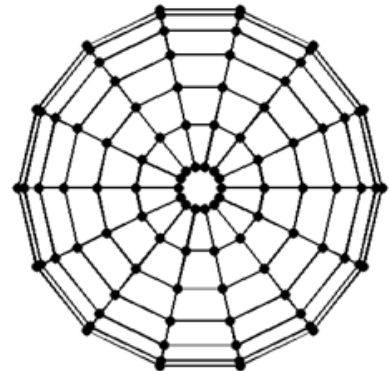
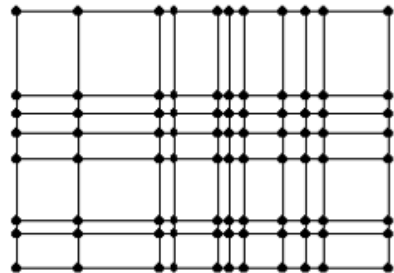
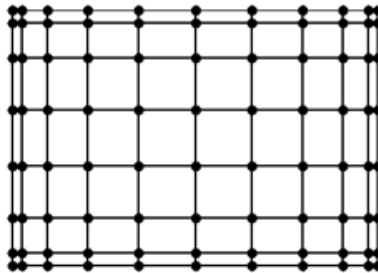
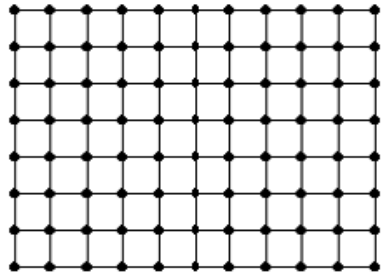
- Unstructured meshes:



Methods: splines

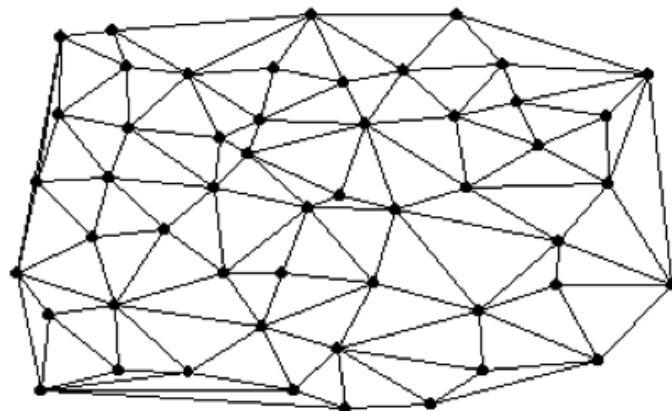
# Grid and mesh-based methods

- Tensor product grids:



Methods: Polynomials, Fourier, splines, etc.

- Unstructured meshes:



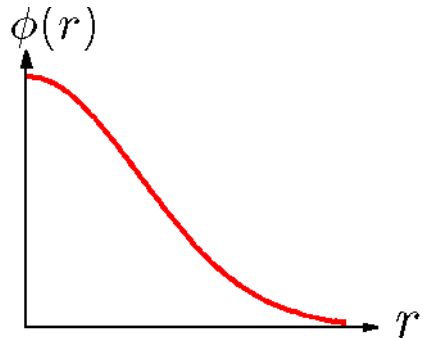
Methods: splines

Our focus:  
Mesh-free methods

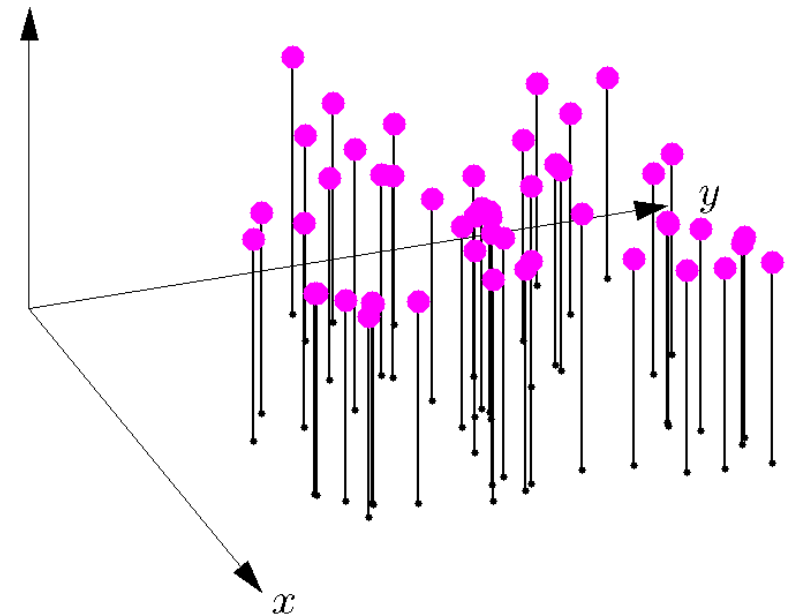
# Radial basis function (RBF) interpolation

Geo Seminar,  
Oct. 21, 2013

Key idea: linear combination of **translates** and **rotations** of a single radial kernel:



$$f \quad X = \{\mathbf{x}_j\}_{j=1}^N \subset \Omega, \quad f|_X = \{f_j\}_{j=1}^N$$



Basic RBF Interpolant for  $\Omega \subseteq \mathbb{R}^2$

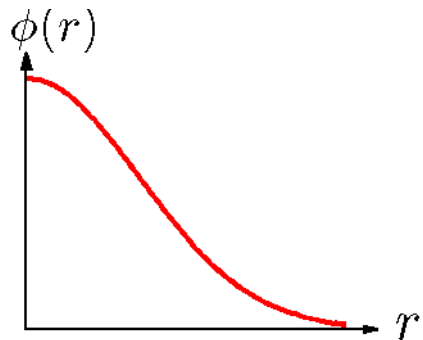
$$s(\mathbf{x}) = \sum_{j=1}^N c_j \phi(\|\mathbf{x} - \mathbf{x}_j\|)$$

$$\text{where } \|\mathbf{x} - \mathbf{x}_j\| = \sqrt{(x - x_j)^2 + (y - y_j)^2}$$

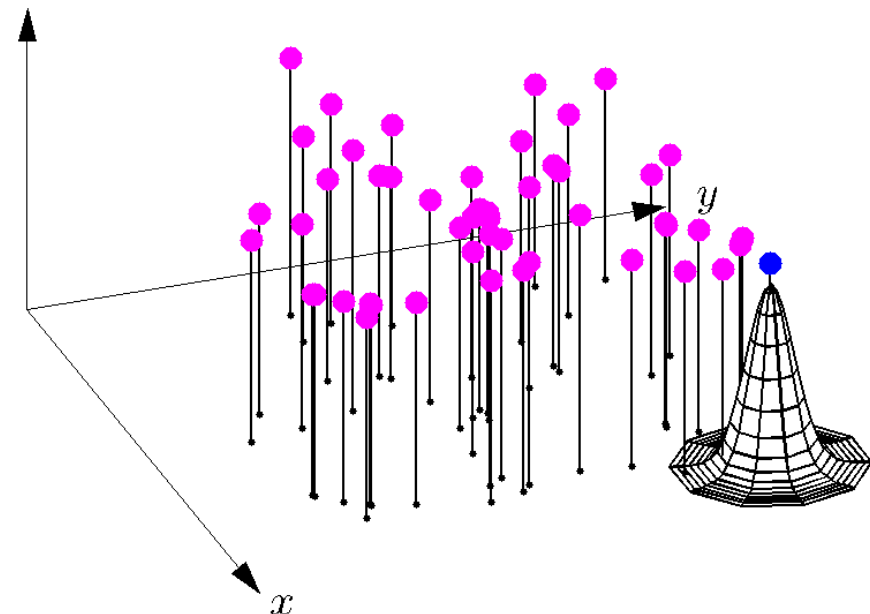
# Radial basis function (RBF) interpolation

Geo Seminar,  
Oct. 21, 2013

Key idea: linear combination of **translates** and **rotations** of a single radial kernel:



$$f \quad X = \{\mathbf{x}_j\}_{j=1}^N \subset \Omega, \quad f|_X = \{\mathbf{f}_j\}_{j=1}^N$$



Basic RBF Interpolant for  $\Omega \subseteq \mathbb{R}^2$

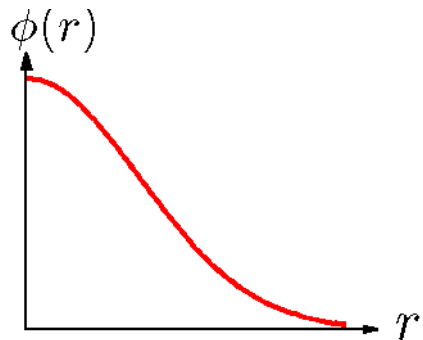
$$s(\mathbf{x}) = \sum_{j=1}^N c_j \phi(\|\mathbf{x} - \mathbf{x}_j\|)$$

$$\text{where } \|\mathbf{x} - \mathbf{x}_j\| = \sqrt{(x - x_j)^2 + (y - y_j)^2}$$

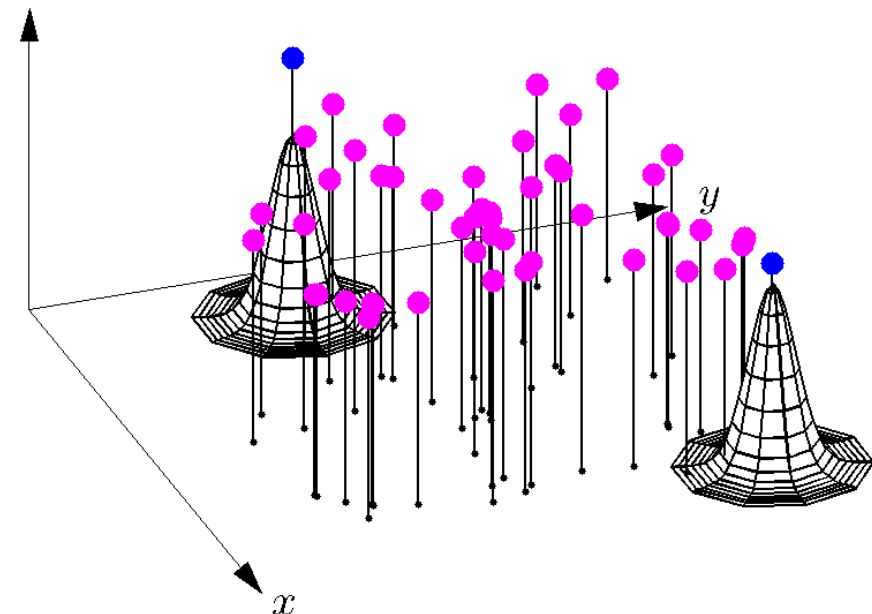
# Radial basis function (RBF) interpolation

Geo Seminar,  
Oct. 21, 2013

Key idea: linear combination of **translates** and **rotations** of a single radial kernel:



$$f \quad X = \{\mathbf{x}_j\}_{j=1}^N \subset \Omega, \quad f|_X = \{\mathbf{f}_j\}_{j=1}^N$$



Basic RBF Interpolant for  $\Omega \subseteq \mathbb{R}^2$

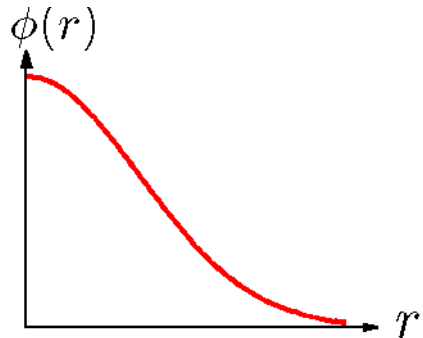
$$s(\mathbf{x}) = \sum_{j=1}^N c_j \phi(\|\mathbf{x} - \mathbf{x}_j\|)$$

$$\text{where } \|\mathbf{x} - \mathbf{x}_j\| = \sqrt{(x - x_j)^2 + (y - y_j)^2}$$

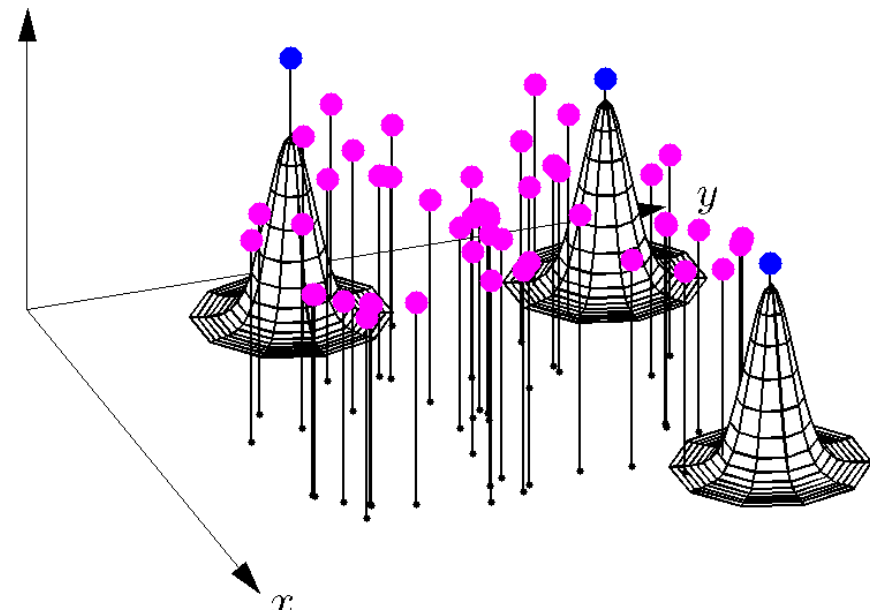
# Radial basis function (RBF) interpolation

Geo Seminar,  
Oct. 21, 2013

Key idea: linear combination of **translates** and **rotations** of a single radial kernel:



$$f \quad X = \{\mathbf{x}_j\}_{j=1}^N \subset \Omega, \quad f|_X = \{\mathbf{f}_j\}_{j=1}^N$$



Basic RBF Interpolant for  $\Omega \subseteq \mathbb{R}^2$

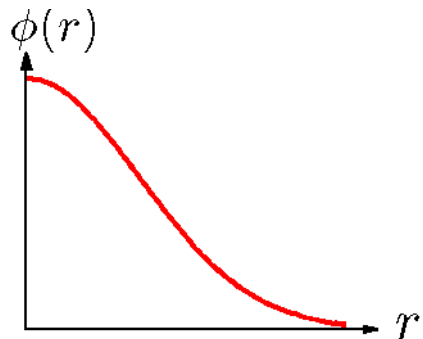
$$s(\mathbf{x}) = \sum_{j=1}^N c_j \phi(\|\mathbf{x} - \mathbf{x}_j\|)$$

$$\text{where } \|\mathbf{x} - \mathbf{x}_j\| = \sqrt{(x - x_j)^2 + (y - y_j)^2}$$

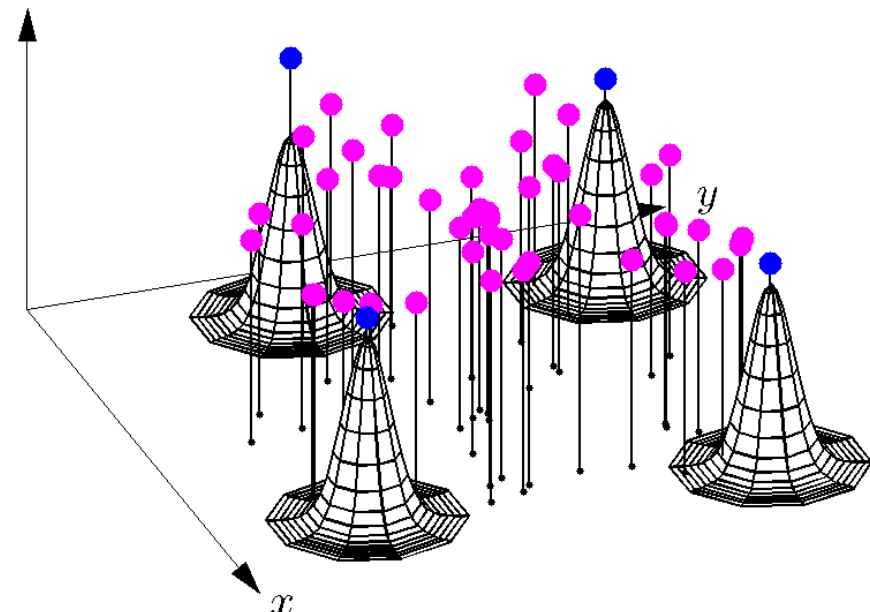
# Radial basis function (RBF) interpolation

Geo Seminar,  
Oct. 21, 2013

Key idea: linear combination of **translates** and **rotations** of a single radial kernel:



$$f \quad X = \{\mathbf{x}_j\}_{j=1}^N \subset \Omega, \quad f|_X = \{\mathbf{f}_j\}_{j=1}^N$$



Basic RBF Interpolant for  $\Omega \subseteq \mathbb{R}^2$

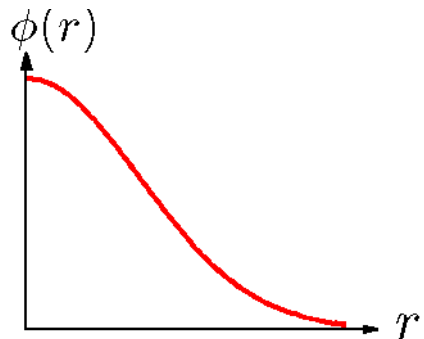
$$s(\mathbf{x}) = \sum_{j=1}^N c_j \phi(\|\mathbf{x} - \mathbf{x}_j\|)$$

$$\text{where } \|\mathbf{x} - \mathbf{x}_j\| = \sqrt{(x - x_j)^2 + (y - y_j)^2}$$

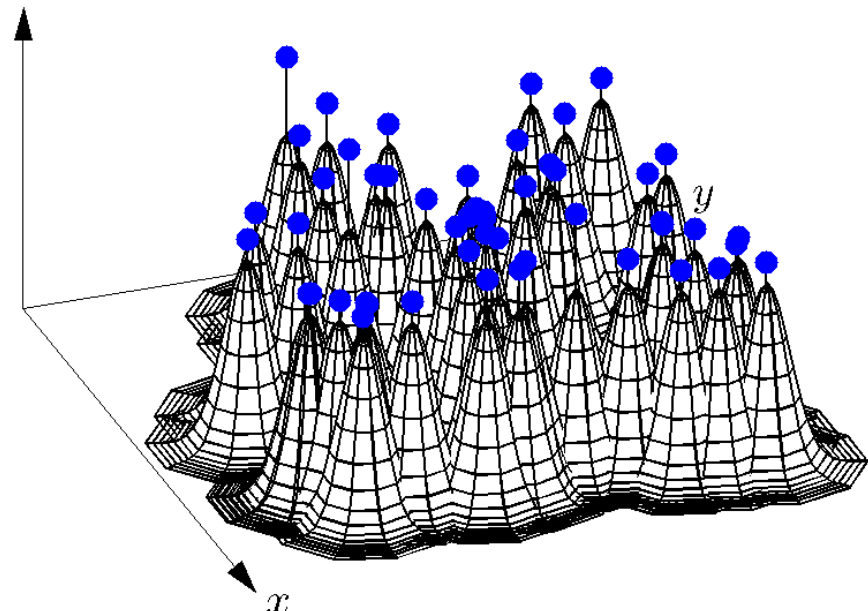
# Radial basis function (RBF) interpolation

Geo Seminar,  
Oct. 21, 2013

Key idea: linear combination of **translates** and **rotations** of a single radial kernel:



$$f \quad X = \{\mathbf{x}_j\}_{j=1}^N \subset \Omega, \quad f|_X = \{\mathbf{f}_j\}_{j=1}^N$$



Basic RBF Interpolant for  $\Omega \subseteq \mathbb{R}^2$

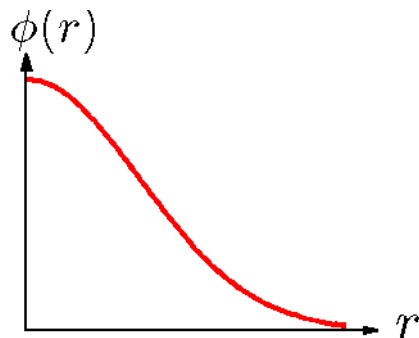
$$s(\mathbf{x}) = \sum_{j=1}^N c_j \phi(\|\mathbf{x} - \mathbf{x}_j\|)$$

$$\text{where } \|\mathbf{x} - \mathbf{x}_j\| = \sqrt{(x - x_j)^2 + (y - y_j)^2}$$

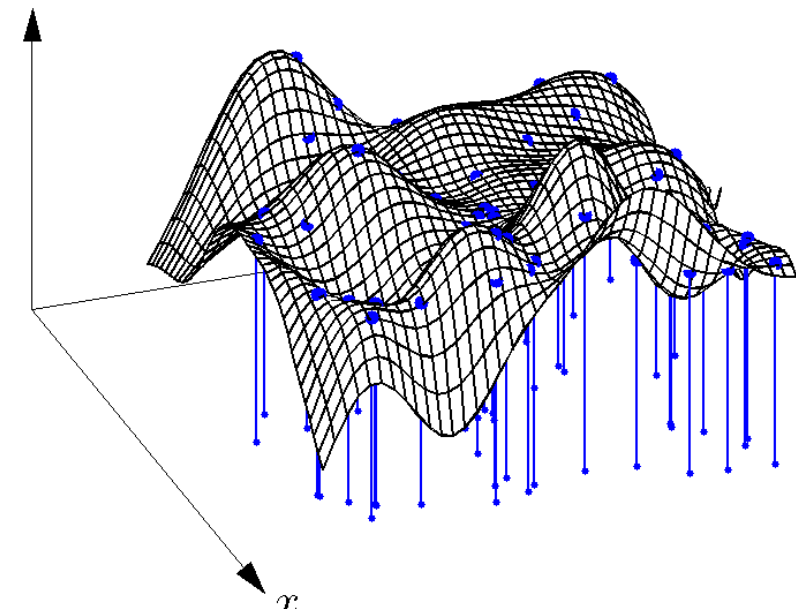
# Radial basis function (RBF) interpolation

Geo Seminar,  
Oct. 21, 2013

Key idea: linear combination of **translates** and **rotations** of a single radial kernel:



$$f \quad X = \{\mathbf{x}_j\}_{j=1}^N \subset \Omega, \quad f|_X = \{\mathbf{f}_j\}_{j=1}^N$$



Basic RBF Interpolant for  $\Omega \subseteq \mathbb{R}^2$

$$s(\mathbf{x}) = \sum_{j=1}^N c_j \phi(\|\mathbf{x} - \mathbf{x}_j\|)$$

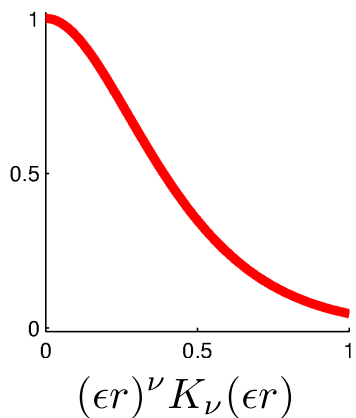
Linear system for determining the interpolation coefficients

$$\underbrace{\begin{bmatrix} \phi(\|\mathbf{x}_1 - \mathbf{x}_1\|) & \phi(\|\mathbf{x}_1 - \mathbf{x}_2\|) & \cdots & \phi(\|\mathbf{x}_1 - \mathbf{x}_N\|) \\ \phi(\|\mathbf{x}_2 - \mathbf{x}_1\|) & \phi(\|\mathbf{x}_2 - \mathbf{x}_2\|) & \cdots & \phi(\|\mathbf{x}_2 - \mathbf{x}_N\|) \\ \vdots & \vdots & \ddots & \vdots \\ \phi(\|\mathbf{x}_N - \mathbf{x}_1\|) & \phi(\|\mathbf{x}_N - \mathbf{x}_2\|) & \cdots & \phi(\|\mathbf{x}_N - \mathbf{x}_N\|) \end{bmatrix}}_{A_X} \underbrace{\begin{bmatrix} c_1 \\ c_2 \\ \vdots \\ c_N \end{bmatrix}}_c = \underbrace{\begin{bmatrix} f_1 \\ f_2 \\ \vdots \\ f_N \end{bmatrix}}_f$$

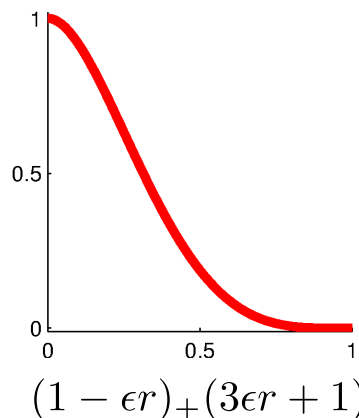
$A_X$  is guaranteed to be **positive definite** if  $\phi$  is positive definite.

# Example of radial functions $\phi(r)$

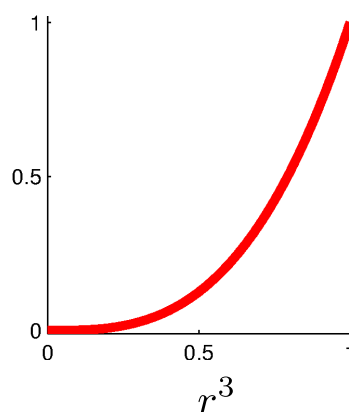
Matérn



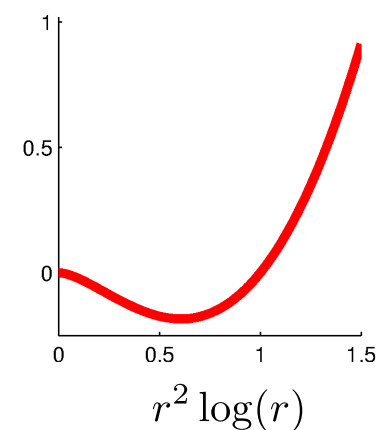
Wendland



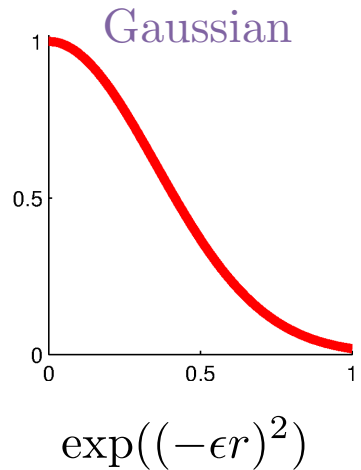
Cubic



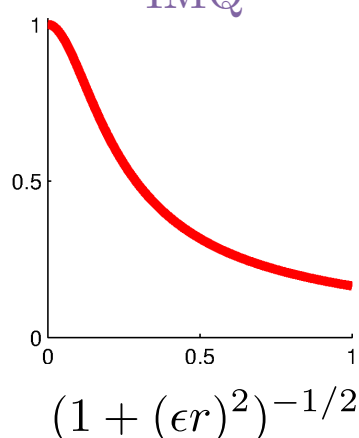
Thin plate spline



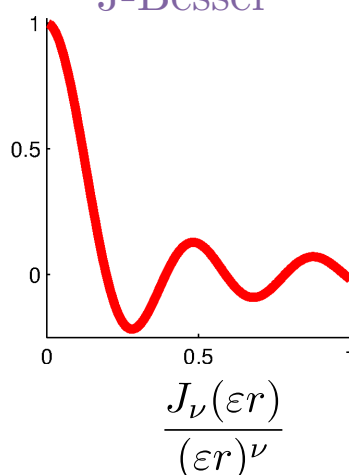
Gaussian



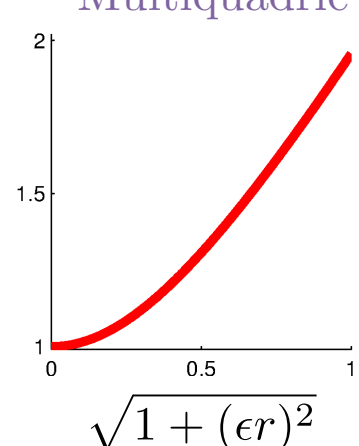
IMQ



J-Bessel



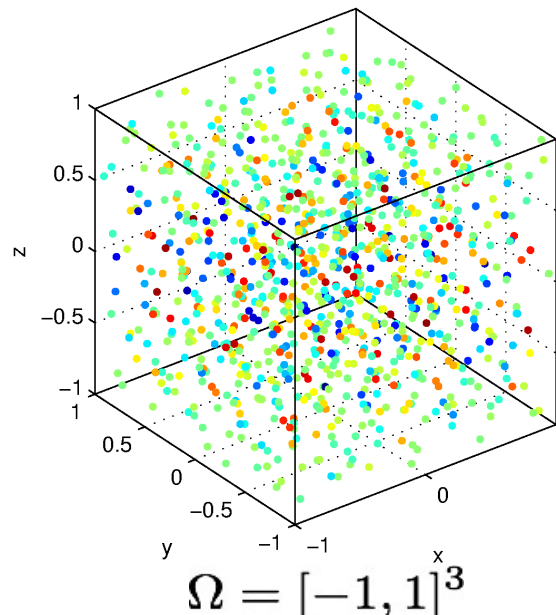
Multiquadric



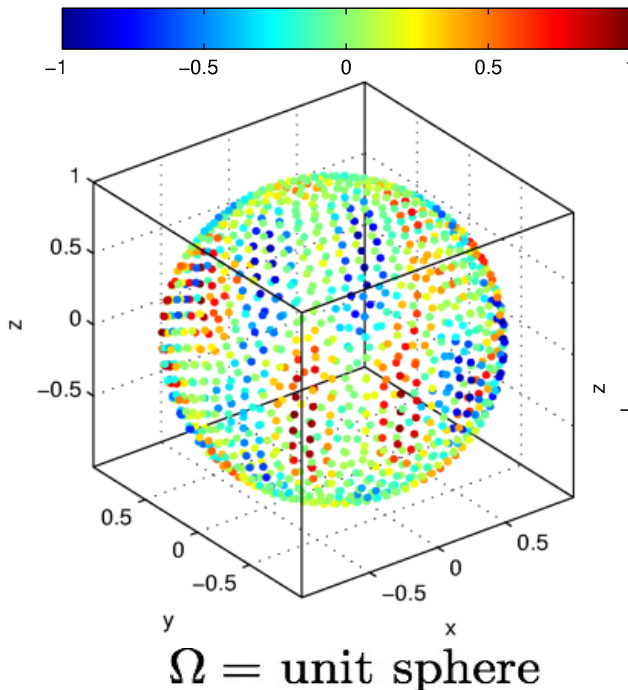
- Reconstruction properties depend on the **smoothness of the data** as well as the **smoothness of the radial function**.

- Consider interpolation of  $f$  from a set of scattered nodes  $X$  on  $\Omega \subset \mathbb{R}^d$

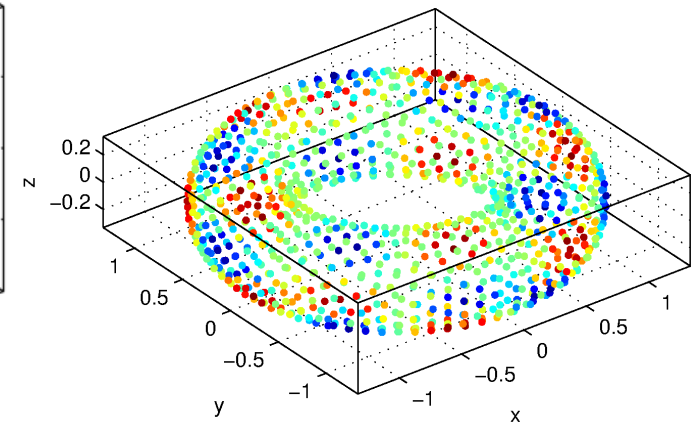
Examples:



$$\Omega = [-1, 1]^3$$



$$\Omega = \text{unit sphere}$$



$$\Omega = \text{a torus}$$

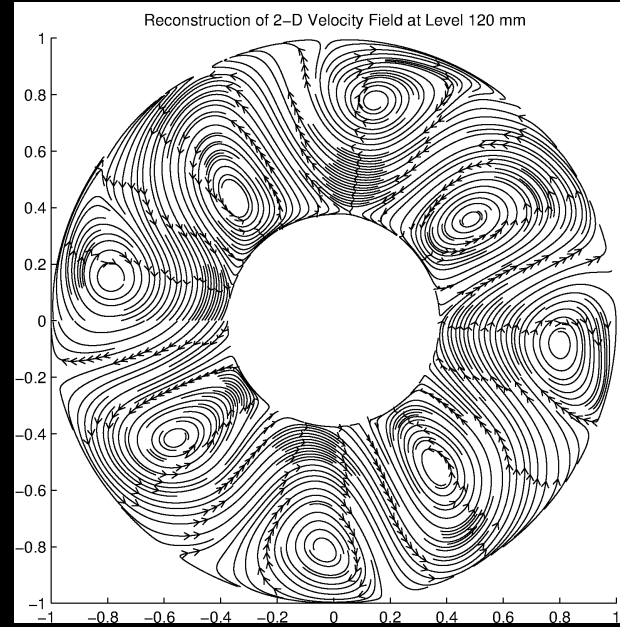
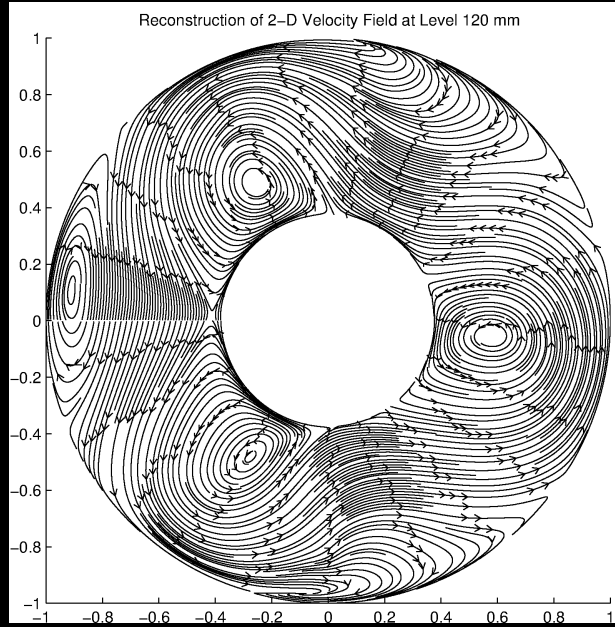
- No special changes are required to construct the RBF interpolant:

$$s(\mathbf{x}) = \sum_{j=1}^N c_j \phi(\|\mathbf{x} - \mathbf{x}_j\|)$$

- RBFs can be adapted very easily to many types of geometries.
- They can also be customized for many different types of applications.

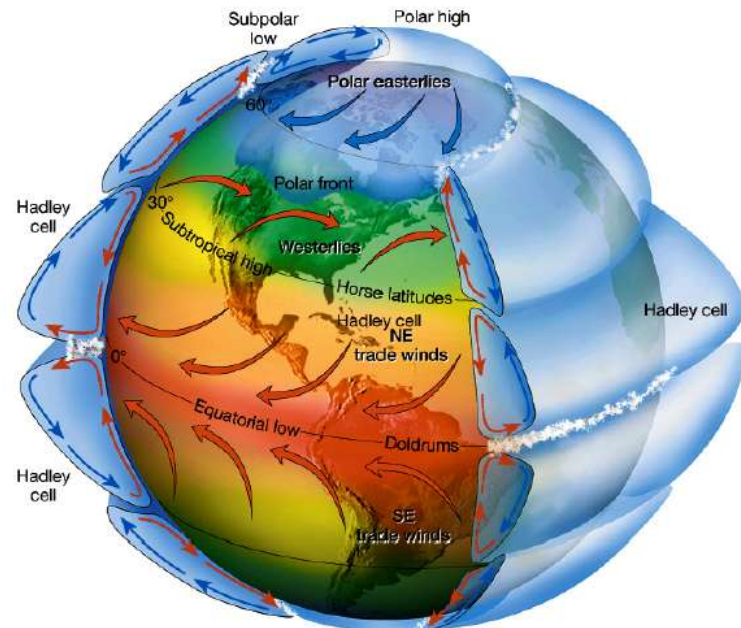
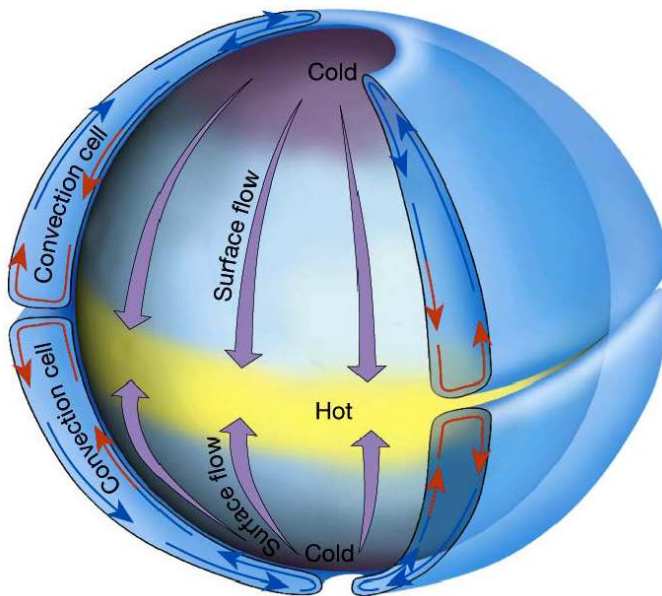
---

# Approximation and decomposition of particle image velocimetry (PIV) data: Differentially heated rotating annulus.



# Baroclinic instability

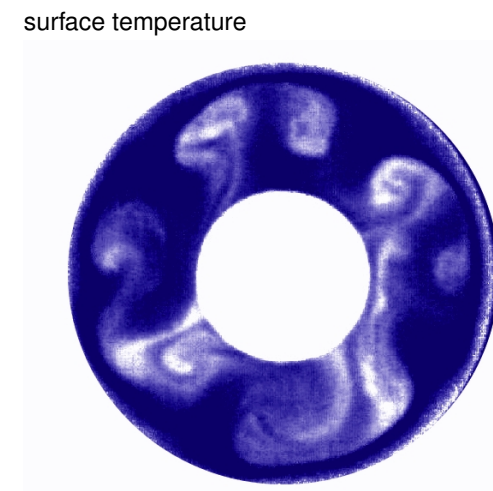
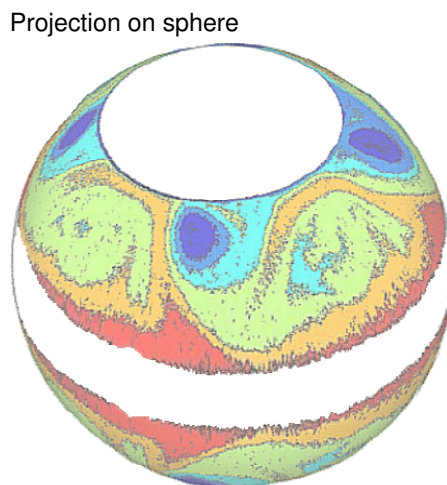
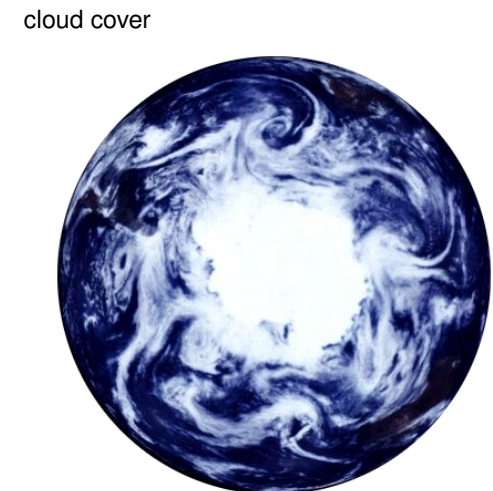
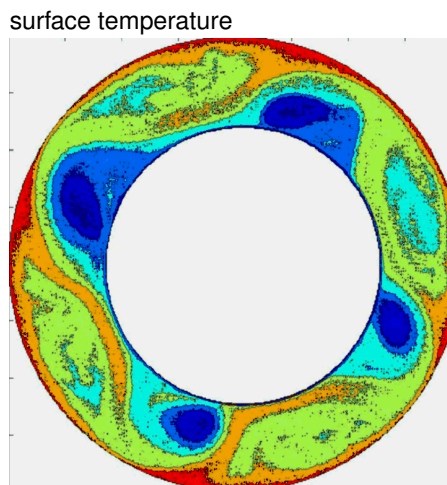
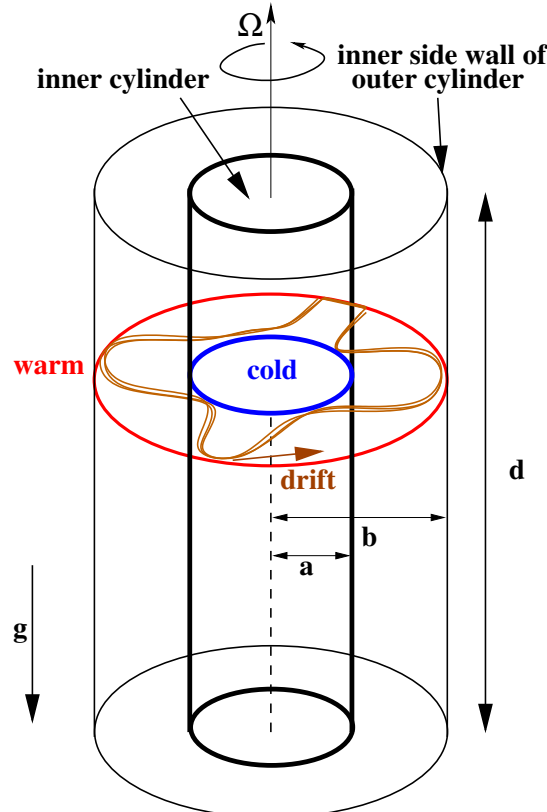
- Joint work with Uwe Harlander, Department Aerodynamics and Fluid Mechanics, BTU Cottbus.  
U. Harlander, Th. von Larcher, G.B. Wright, M. Hoff, K. Alexandrov, C. Egbers. Orthogonal decomposition methods to analyze PIV, LDA and thermography data of a thermally driven rotating annulus laboratory experiment. In press (2014 expected publication)
- DFG program MetStröm: Multiple Scales in Fluid Mechanics and Meteorology
- Atmospheric general circulation:



Source: Vera Schlanger - Hungarian Meteorological Service

# Differentially heated rotating annulus

- Accepted laboratory experiment for large scale flow in the mid-latitudes.



Parameters:

$$\begin{aligned}\Omega &= \text{rotation rate} \\ \Delta T &= T_{\text{outer}} - T_{\text{inner}} \\ b - a &= \text{width annulus} \\ d &= \text{height annulus}\end{aligned}$$

# Equations, numbers, experimental setup

## Governing equations:

$$\frac{\partial \mathbf{u}}{\partial t} + \mathbf{u} \cdot \nabla \mathbf{u} = -\nabla p + \Delta \mathbf{u}$$

–  $\text{Ra}\phi\mathbf{k} - \text{Ta}^{1/2}\mathbf{k} \times \mathbf{u}$

$$\frac{\partial \phi}{\partial t} + \mathbf{u} \cdot \nabla \phi = \frac{1}{\text{Pa}} \Delta \phi$$

$\nabla \cdot \mathbf{u} = 0$

## Non-dimensional numbers

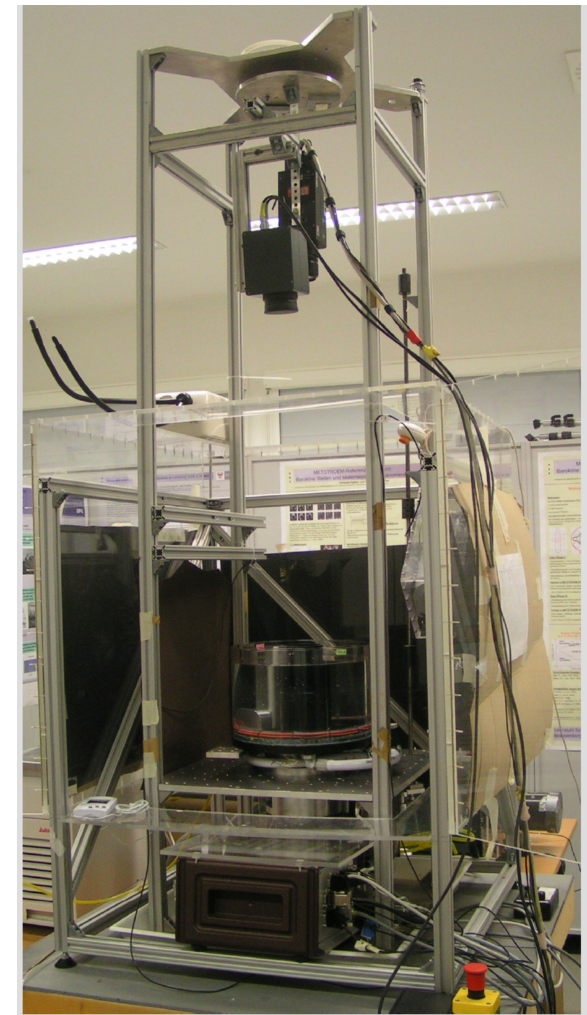
Taylor	$\text{Ta}$	$\frac{4\Omega^2(b-a)^4}{\nu^2}$
--------	-------------	----------------------------------

Rayleigh	$\text{Ra}$	$\frac{g\alpha\Delta T(b-a)^3}{\kappa\nu}$
----------	-------------	--

Prandtl	$\text{Pr}$	$\frac{\nu}{\kappa}$
---------	-------------	----------------------

Modified Taylor	$\text{Ta}'$	$\frac{b-a}{d} \text{Ta}$
-----------------	--------------	---------------------------

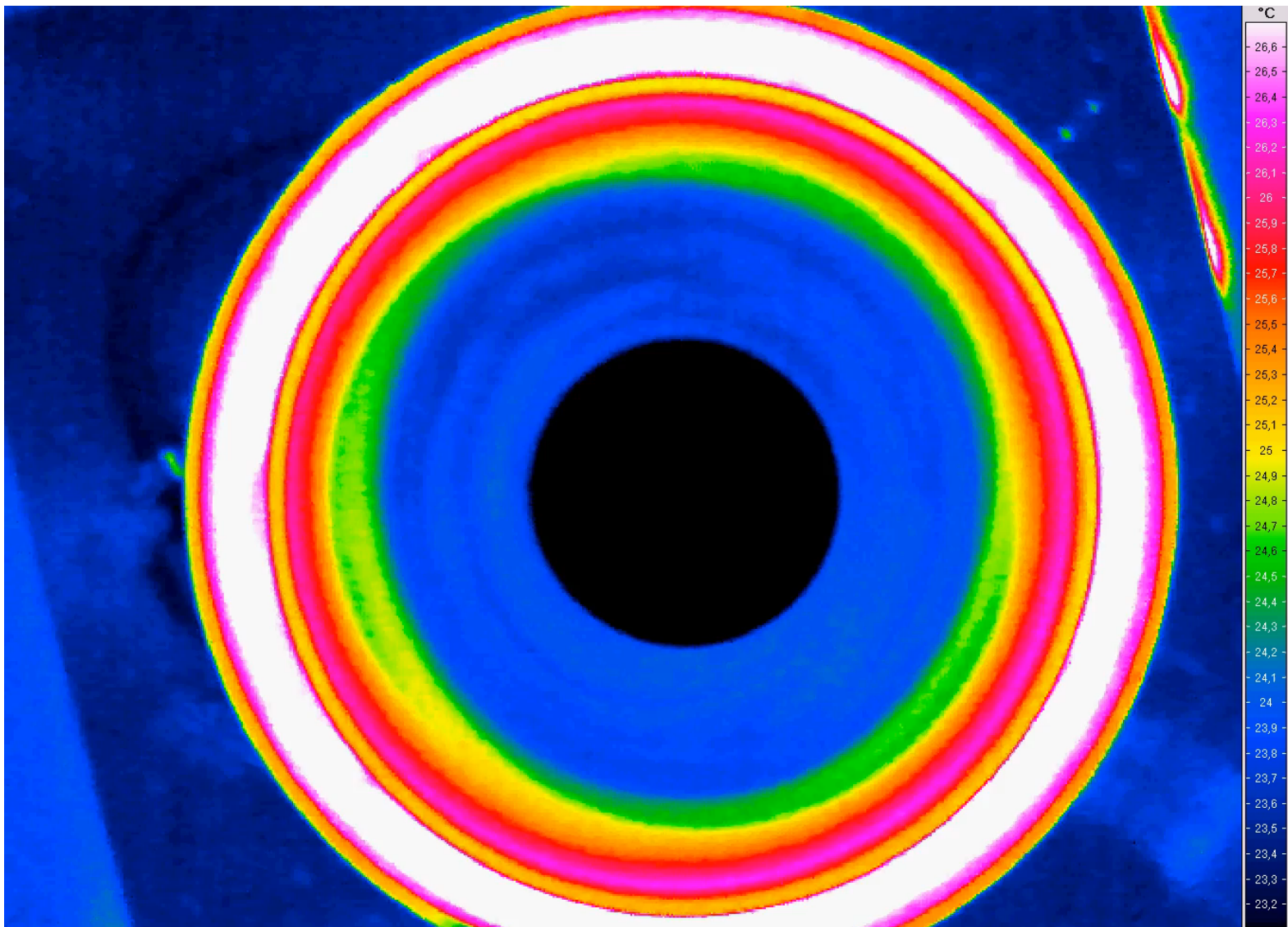
Thermal Rosby	$\text{Ro}$	$4 \frac{\text{Ra}}{\text{PrTa}}$
---------------	-------------	-----------------------------------



Actual experiment at BTU  
Cottbus.

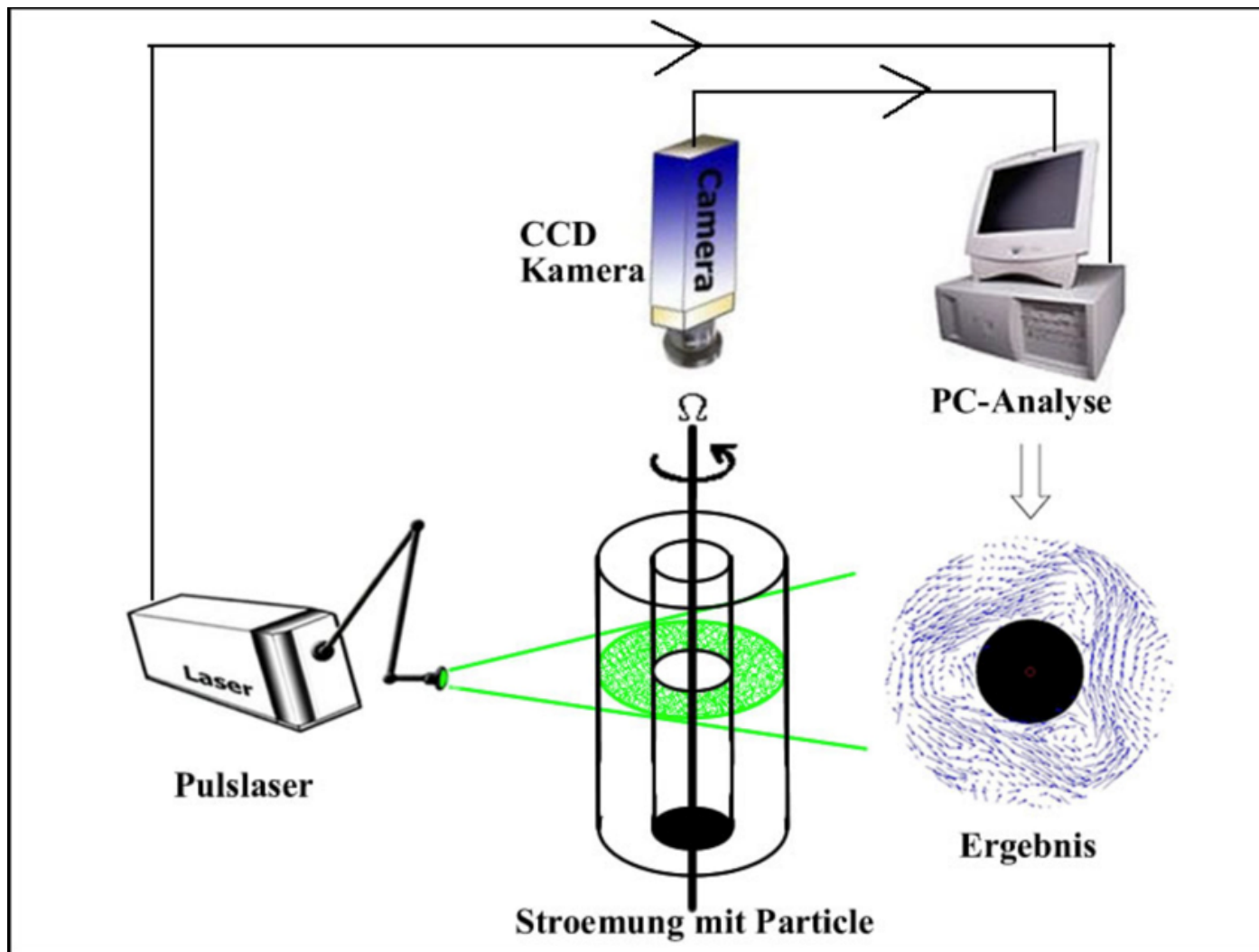
# Movie of spin-up to a 3-wave pattern

	$\Omega$ [rpm]	$\Delta T$ [K]	$Ta$	$Ro_{th}$	$b - a$ [mm]	d [mm]
exp	6	5.1	$1.55 \cdot 10^7$	0.79	75	135



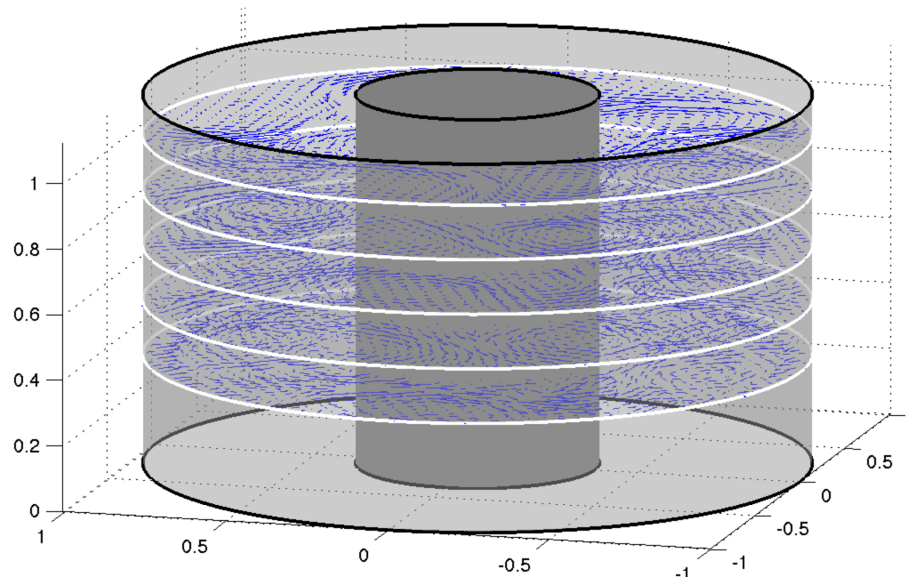
# Fluid velocity measurements: PIV

- At various levels of the tank, horizontal velocity measurements of the fluid are obtained by Particle Image Velocimetry (PIV).

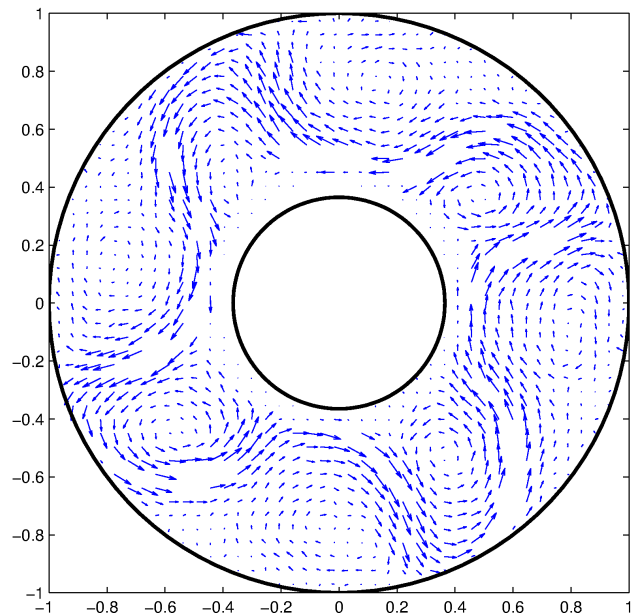


# Data analysis problems

Velocity data at all levels:



Velocity data at top level:



**First problem:**

Reconstruct the full 3D field from the various horizontal slices.

- a) Reconstruct the 2D field on each horizontal slice.
- b) Compute divergence of the reconstructed field.
- c) Use incompressibility of the full 3D field to recover the vertical velocity component:

$$w_z = -(u_x + v_y) \implies w = - \int_{z_0}^z (u_x + v_y) dz$$

Challenge: Data is scattered and contains noise.

# Data analysis problems

Second (and more interesting) problem:

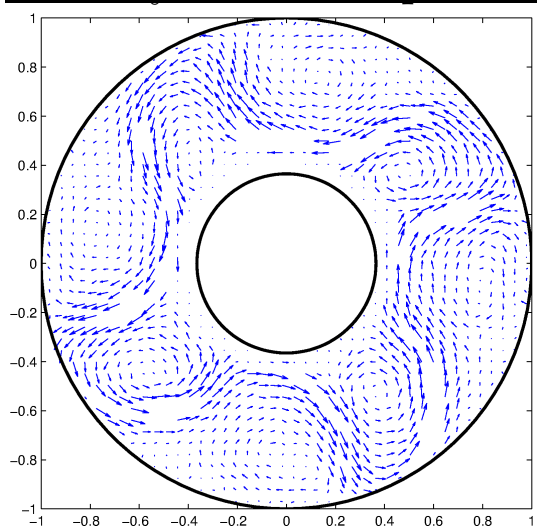
Compute the Helmholtz-Hodge decomposition of the 2D horizontal fields.

Recall: Helmholtz-Hodge theorem states any sufficiently smooth vector field  $\mathbf{u}$  can be decomposed as follows:

$$\begin{aligned}\mathbf{u} &= \mathbf{u}_{\text{div}} + \mathbf{u}_{\text{curl}} \\ &= \nabla \times (\psi \mathbf{k}) + \nabla \phi \quad (\text{for 2D field})\end{aligned}$$

Decomposition is unique if appropriate boundary conditions applied.

Velocity data at top level:



Importance: These two fields can be used to discriminate different wave-types:

Baroclinic and Rossby waves are **div-free**, while inertial-gravity waves are not.

**Challenge**: Data is scattered and contains noise.

# Property conserving approximations

## Key idea:

Use a reconstruction that mimics the Helmholtz-Hodge decomposition theorem.

## Notation:

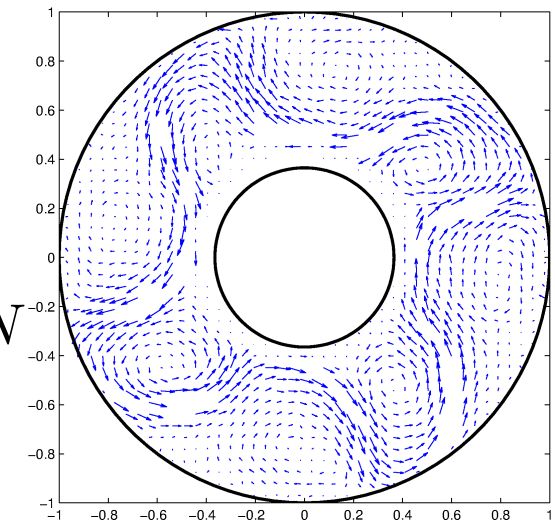
$\mathbf{u}_j = (u_j, v_j)$  is measured field at  $\mathbf{x}_j$ ,  $j = 1, \dots, N$

$\xi_k$  = nodes on the boundary,  $k = 1, \dots, M$

$\mathbf{n}_k$  = unit outward normal at  $\xi_k$

## Property conserving approximation:

$$\mathbf{s}(\mathbf{x}) = \sum_{j=1}^N \Phi_{\text{div}}(\mathbf{x}, \mathbf{x}_j) \mathbf{a}_j + \sum_{k=1}^M [\Phi_{\text{div}}(\mathbf{x}, \xi_j) \mathbf{n}_k] d_j + \sum_{j=1}^N \Phi_{\text{curl}}(\mathbf{x}, \mathbf{x}_j) \mathbf{a}_j$$



- $\Phi_{\text{div}}$  and  $\Phi_{\text{curl}}$  are 2-by-2 *matrix-valued* functions
- Columns of  $\Phi_{\text{div}}$  are divergence-free
- Columns of  $\Phi_{\text{curl}}$  are curl-free

# Property conserving approximations

Key idea:

Use a reconstruction that mimics the Helmholtz-Hodge decomposition theorem.

Notation:

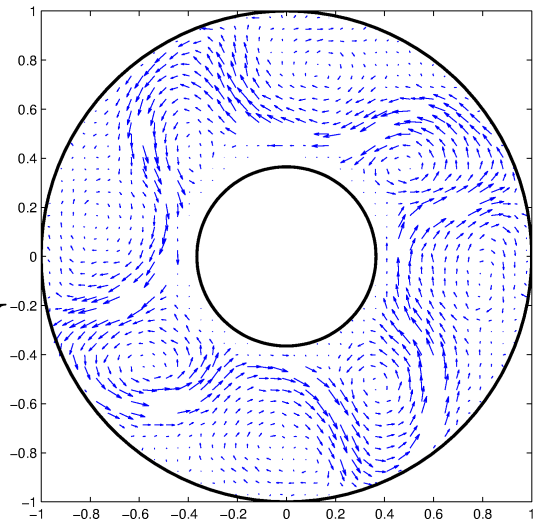
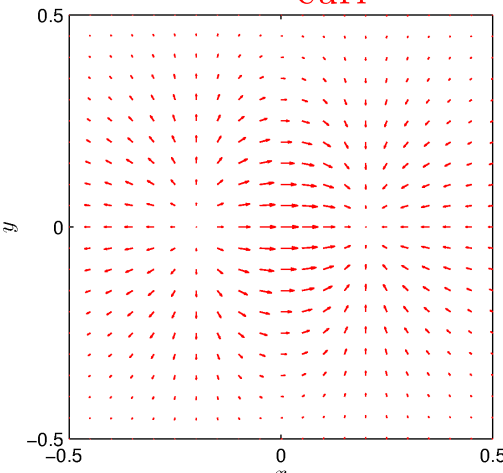
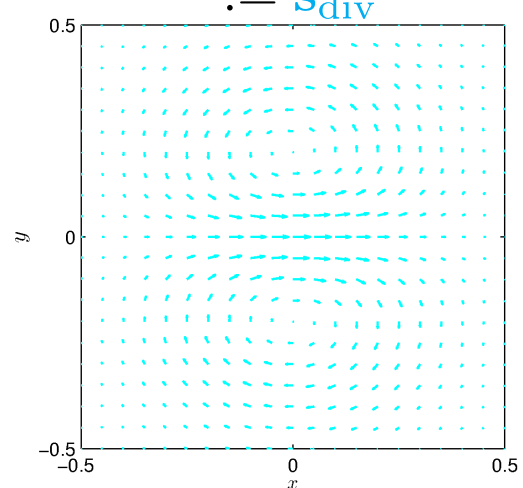
$\mathbf{u}_j = (u_j, v_j)$  is measured field at  $\mathbf{x}_j$ ,  $j = 1, \dots, N$

$\xi_k$  = nodes on the boundary,  $k = 1, \dots, M$

$\mathbf{n}_k$  = unit outward normal at  $\xi_k$

Property conserving approximation:

$$\mathbf{s}(\mathbf{x}) = \underbrace{\sum_{j=1}^N \Phi_{\text{div}}(\mathbf{x}, \mathbf{x}_j) \mathbf{a}_j + \sum_{k=1}^M [\Phi_{\text{div}}(\mathbf{x}, \xi_j) \mathbf{n}_k] d_j}_{:= \mathbf{s}_{\text{div}}} + \underbrace{\sum_{j=1}^N \Phi_{\text{curl}}(\mathbf{x}, \mathbf{x}_j) \mathbf{a}_j}_{:= \mathbf{s}_{\text{curl}}}$$



# Property conserving approximations

Key idea:

Use a reconstruction that mimics the Helmholtz-Hodge decomposition theorem.

Notation:

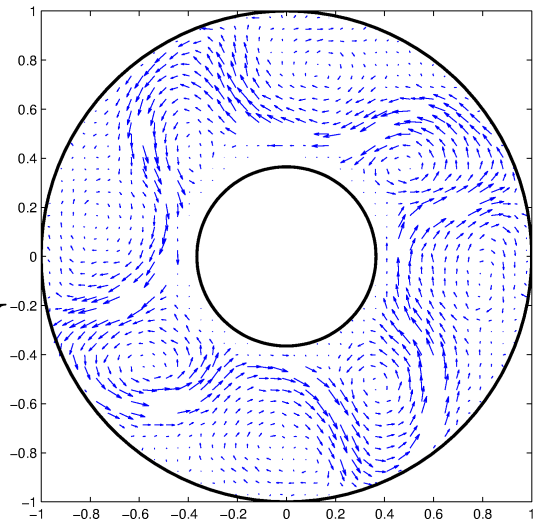
$\mathbf{u}_j = (u_j, v_j)$  is measured field at  $\mathbf{x}_j$ ,  $j = 1, \dots, N$

$\xi_k$  = nodes on the boundary,  $k = 1, \dots, M$

$\mathbf{n}_k$  = unit outward normal at  $\xi_k$

Property conserving approximation:

$$\mathbf{s}(\mathbf{x}) = \underbrace{\sum_{j=1}^N \Phi_{\text{div}}(\mathbf{x}, \mathbf{x}_j) \mathbf{a}_j + \sum_{k=1}^M [\Phi_{\text{div}}(\mathbf{x}, \xi_j) \mathbf{n}_k] d_j}_{:= \mathbf{s}_{\text{div}}} + \underbrace{\sum_{j=1}^N \Phi_{\text{curl}}(\mathbf{x}, \mathbf{x}_j) \mathbf{a}_j}_{:= \mathbf{s}_{\text{curl}}}$$



Constraints for interpolation:

$$\begin{aligned} \mathbf{s}(\mathbf{x}_i) &= \mathbf{u}_i, \quad i = 1, \dots, N, \\ \mathbf{s}_{\text{div}}(\xi_i) \cdot \mathbf{n}_i &= 0, \quad i = 1, \dots, M, \end{aligned}$$

(Leads to a invertible linear system of equations)

# Property conserving approximations

Key idea:

Use a reconstruction that mimics the Helmholtz-Hodge decomposition theorem.

Notation:

$\mathbf{u}_j = (u_j, v_j)$  is measured field at  $\mathbf{x}_j$ ,  $j = 1, \dots, N$

$\xi_k$  = nodes on the boundary,  $k = 1, \dots, M$

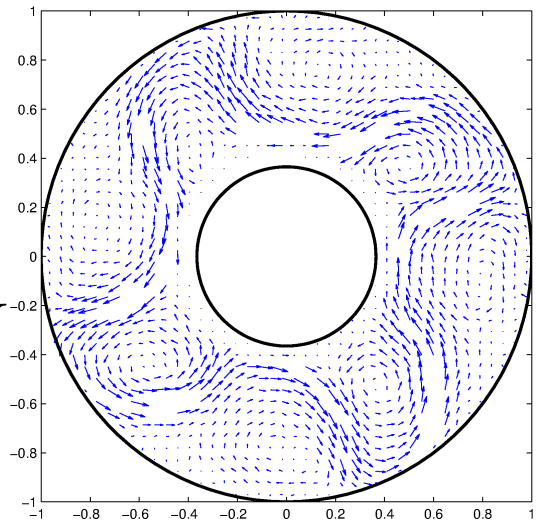
$\mathbf{n}_k$  = unit outward normal at  $\xi_k$

Property conserving approximation:

$$\mathbf{s}(\mathbf{x}) = \underbrace{\sum_{j=1}^N \Phi_{\text{div}}(\mathbf{x}, \mathbf{x}_j) \mathbf{a}_j + \sum_{k=1}^M [\Phi_{\text{div}}(\mathbf{x}, \xi_j) \mathbf{n}_k] d_j}_{:= \mathbf{s}_{\text{div}}} + \underbrace{\sum_{j=1}^N \Phi_{\text{curl}}(\mathbf{x}, \mathbf{x}_j) \mathbf{a}_j}_{:= \mathbf{s}_{\text{curl}}}$$

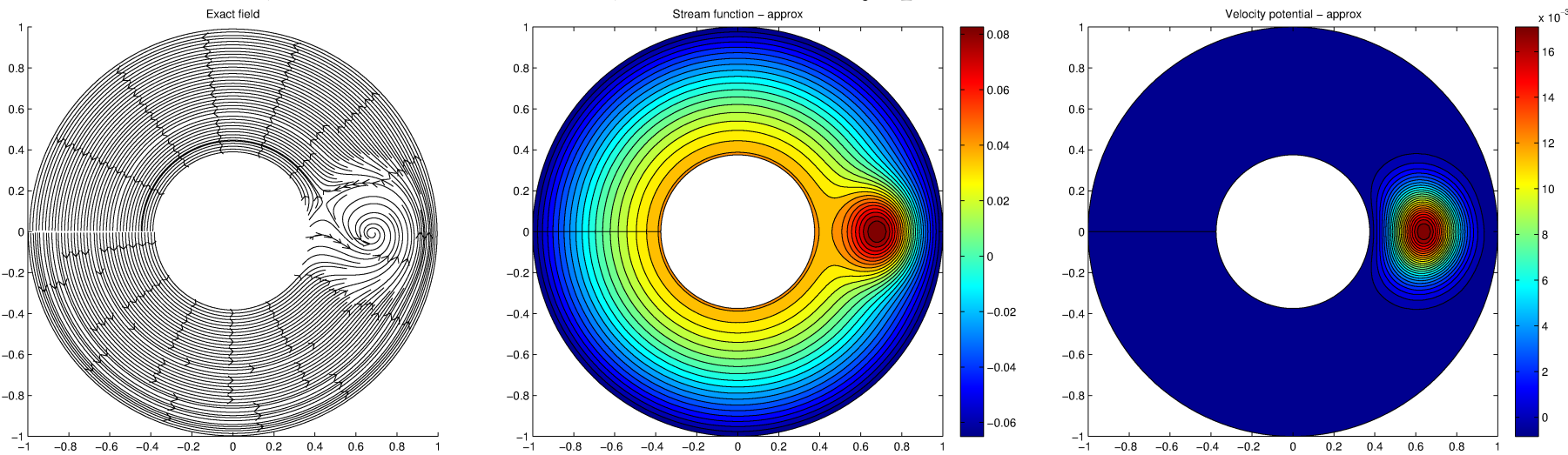
Results:

1.  $\mathbf{s} \approx \mathbf{u}$ ,  $\mathbf{s}_{\text{div}} \approx \mathbf{u}_{\text{div}}$ ,  $\mathbf{s}_{\text{curl}} \approx \mathbf{u}_{\text{curl}}$
2. A stream-function and velocity potential for the fields can be recovered.
3. Low-pass filter can be used to filter the noise.

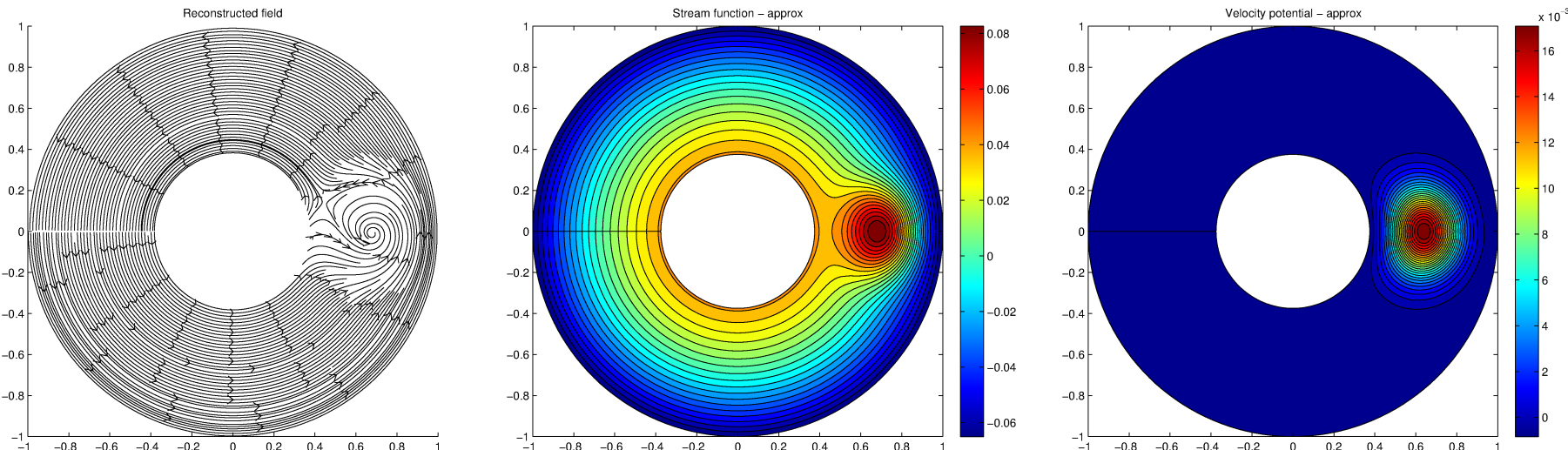


# Example with exact data

- Exact field, stream function, and velocity potential

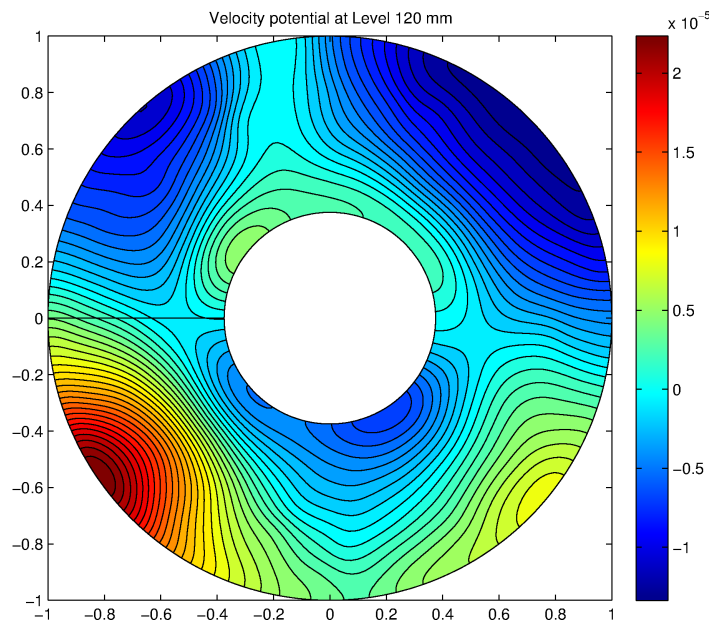
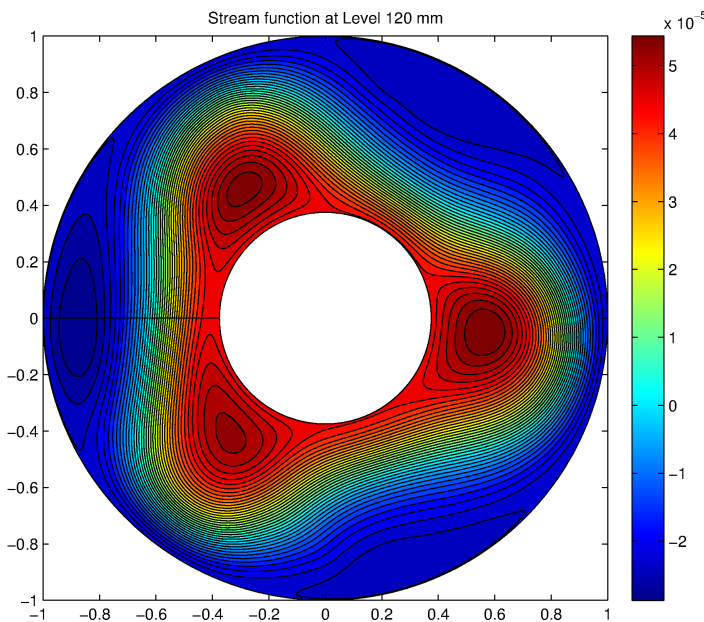
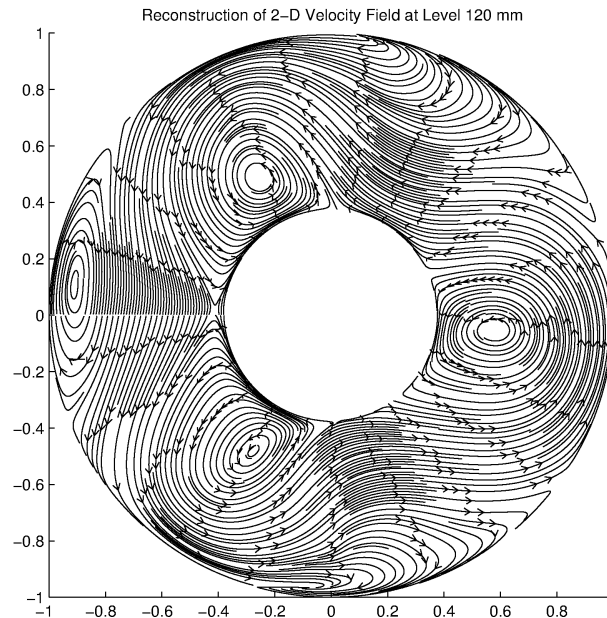
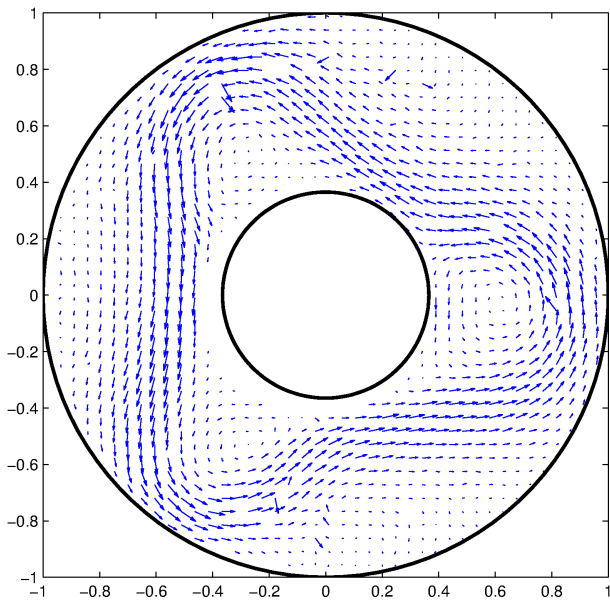


- Reconstructed field, stream function and velocity potential



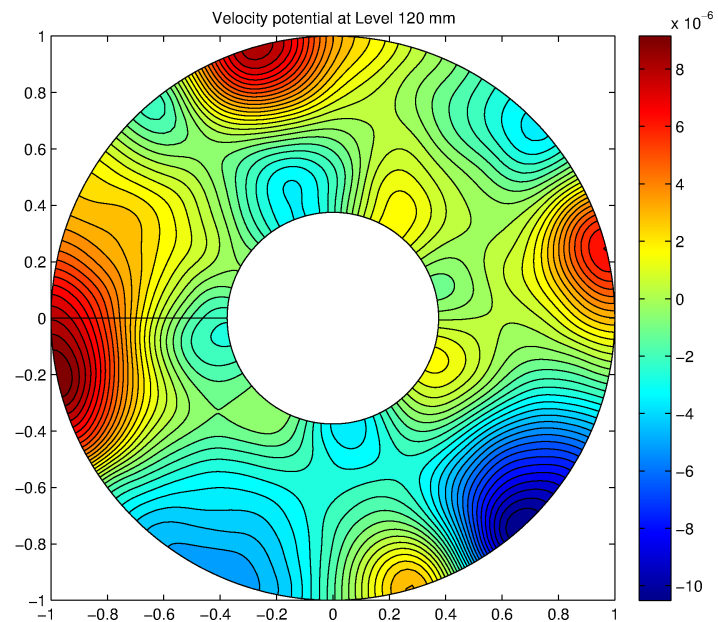
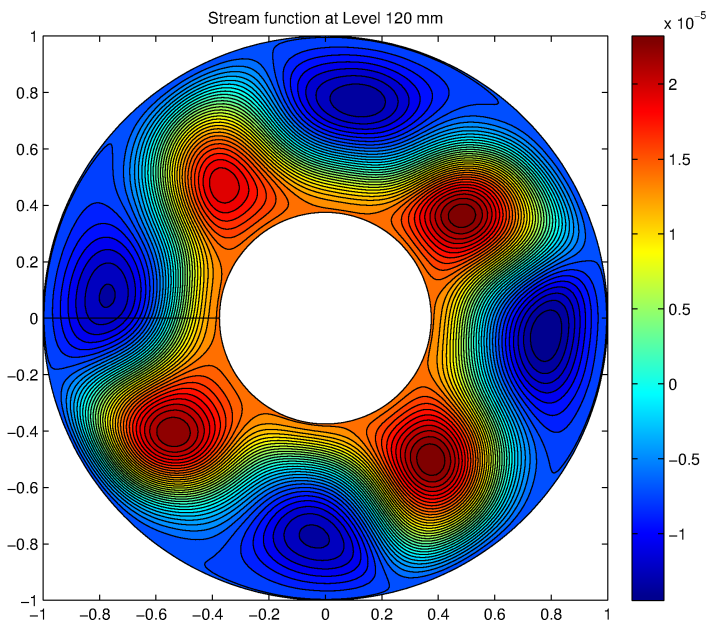
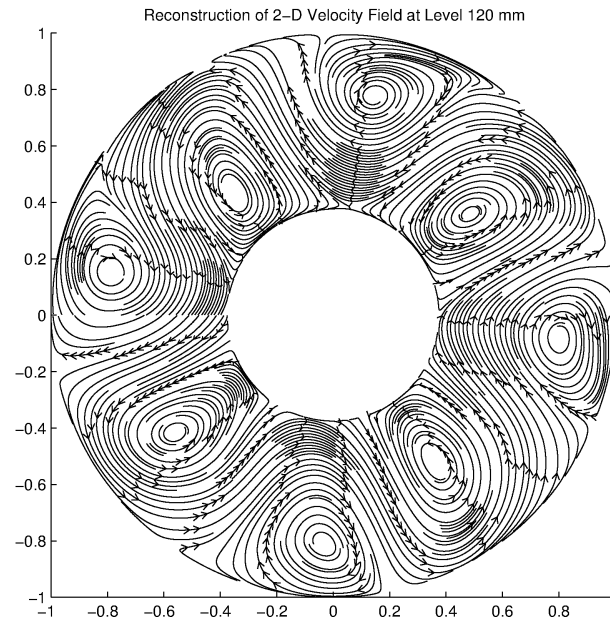
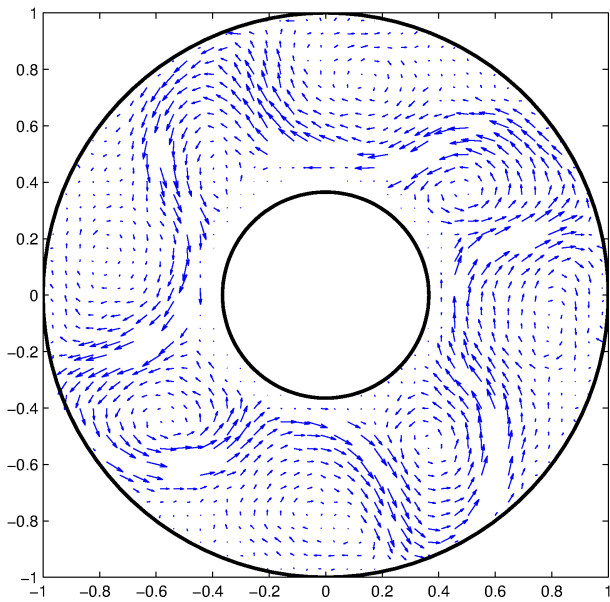
# Decompositions of annulus data: 3-wave

Geo Seminar,  
Oct. 21, 2013



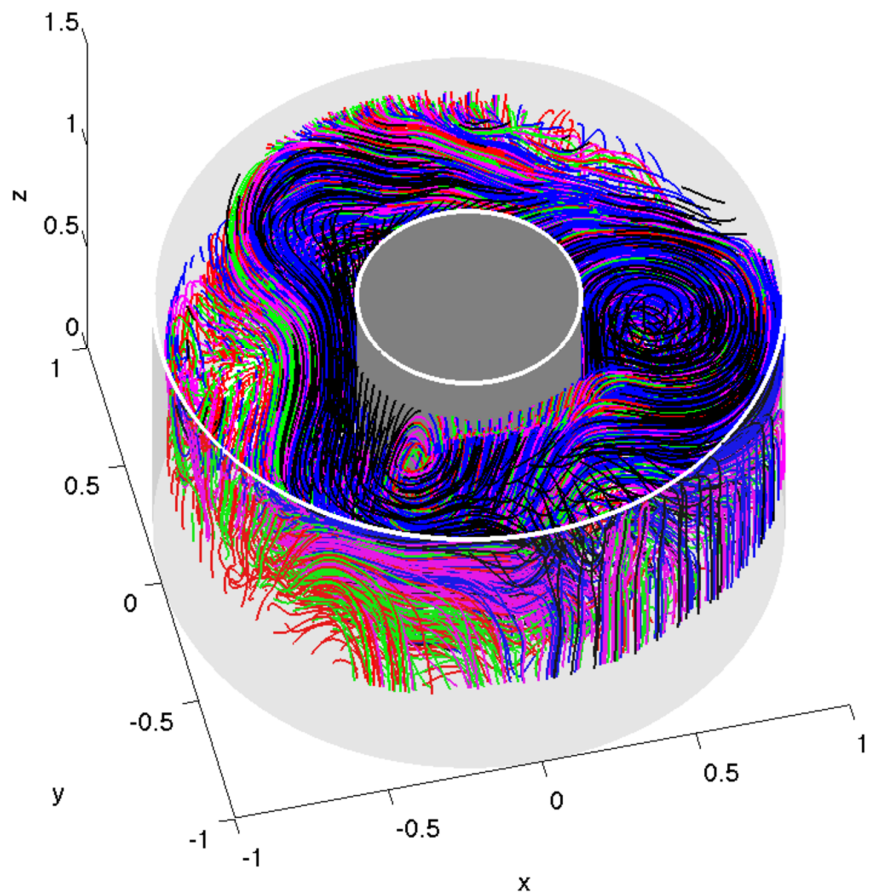
# Decompositions of annulus data: 4-wave

Geo Seminar,  
Oct. 21, 2013

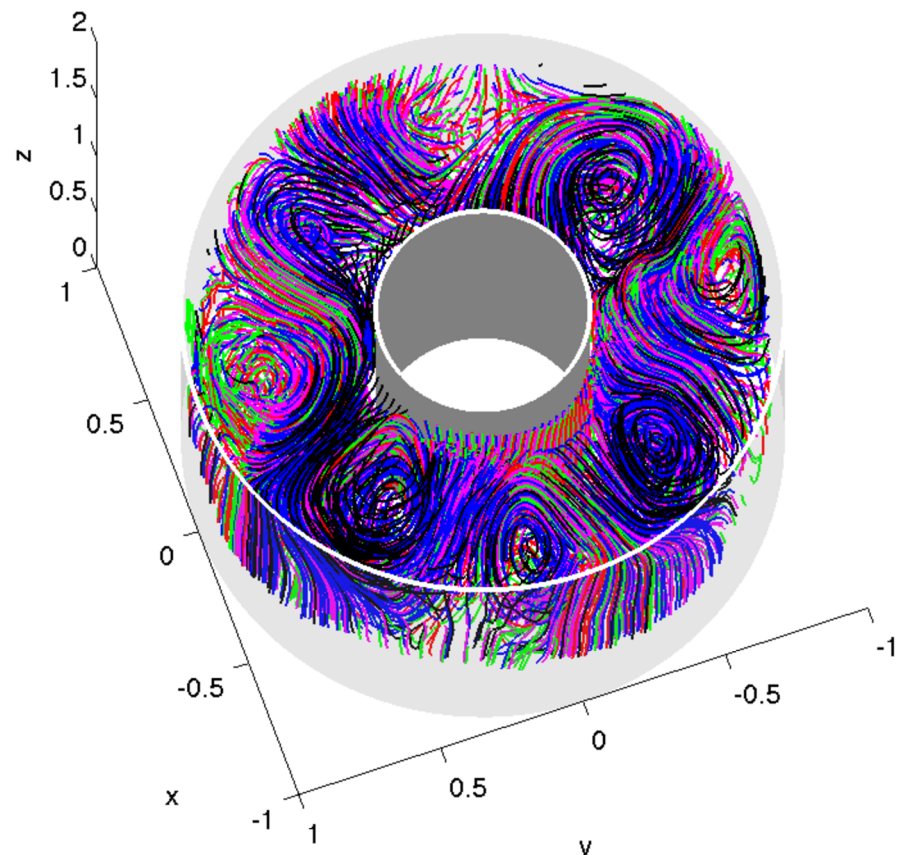


# Full 3D reconstructions of the velocity

3-wave pattern



4-wave pattern



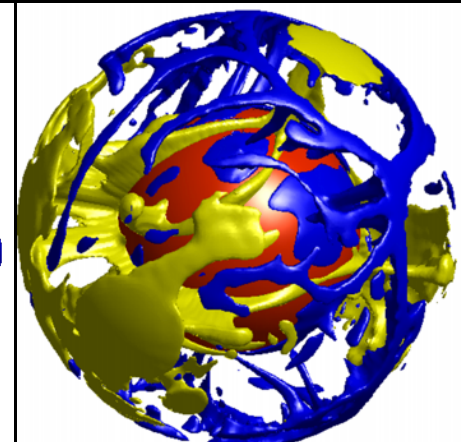
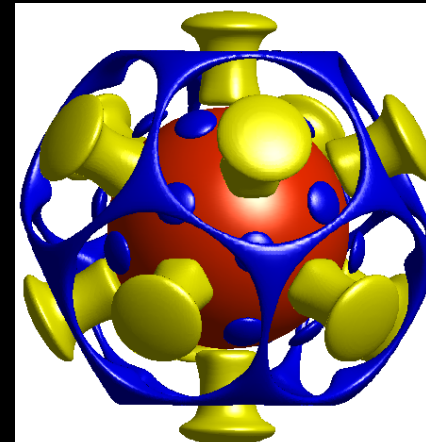
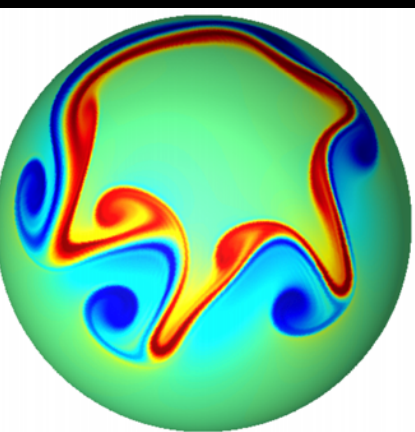
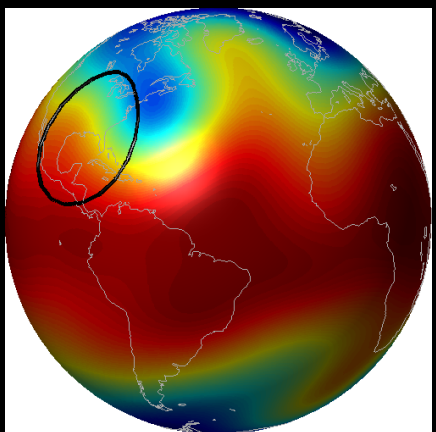
The colors of the streamlines correspond to the vertical levels of the streamline seeds:  
**red=40mm, green=60mm, magenta=80mm, blue=100mm, black=120mm**

# Discussion

- We were unable to detect inertial gravity waves in the curl-free part of the measured field.
  - Reason may be that the resolution was not high enough in the PIV measurements to resolve these parts of the flow.
  - Stereo PIV of the full 3D field may yield better results (tests underway).
- The method did provide a nice way to reconstruct the full 3D flow field from 2D slices of the velocity (something that hadn't been done before).
- More robust noise filter needs to be analyzed.
- Other applications of the decomposition technique?

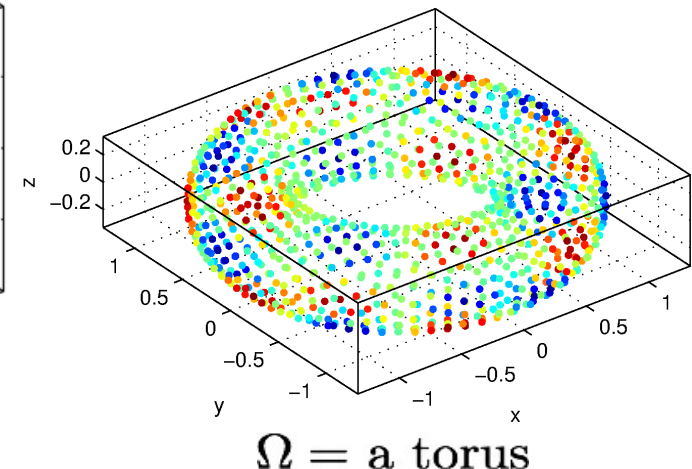
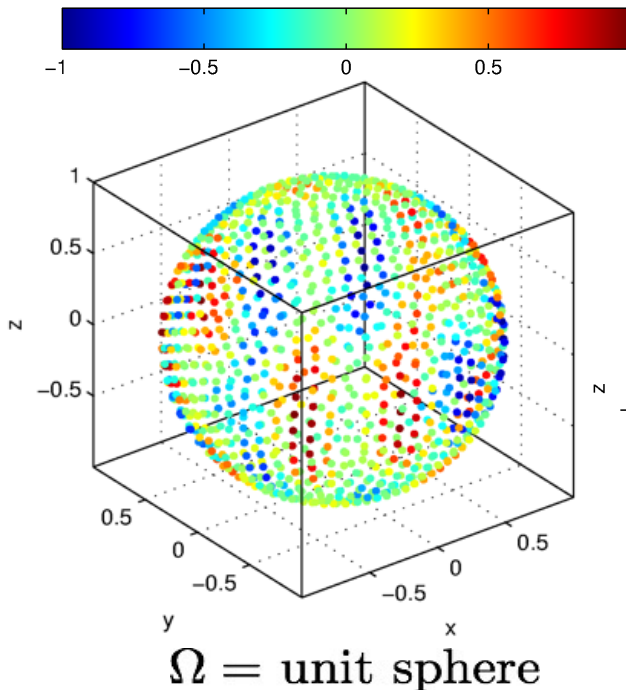
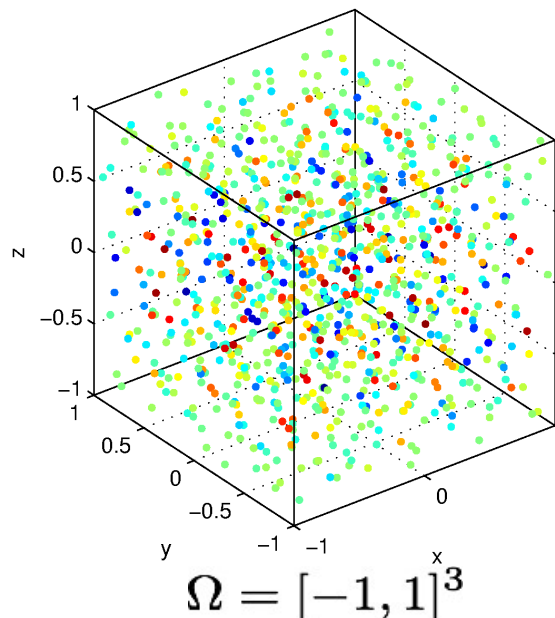
---

# Geophysical modeling and simulation in spherical geometries



- Consider interpolation of  $f$  from a set of scattered nodes  $X$  on  $\Omega \subset \mathbb{R}^d$

Examples:



- No special changes are required to construct the RBF interpolant:

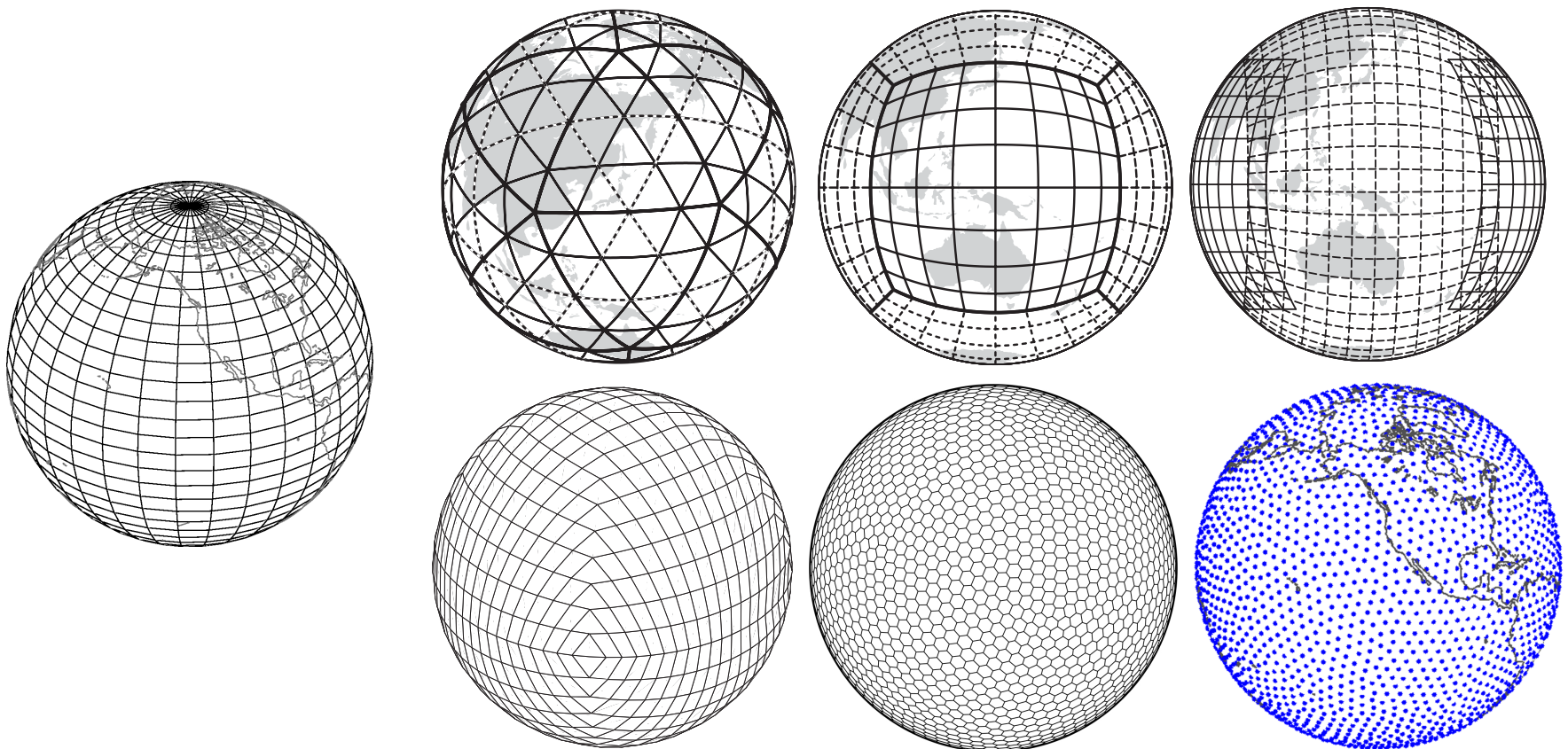
$$s(\mathbf{x}) = \sum_{j=1}^N c_j \phi(\|\mathbf{x} - \mathbf{x}_j\|)$$

- RBFs can be adapted very easily to many types of geometries.

# Grids, meshes, nodes, used in large scale models

Geo Seminar,  
Oct. 21, 2013

- Grids/meshes/nodes used in methods for large-scale applications:

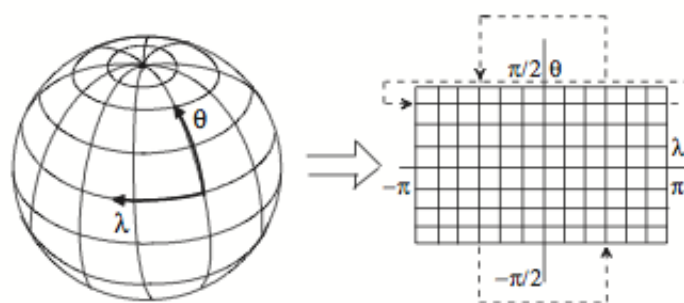


- Types of discretization methods in use:
  - Finite-difference, finite-element, finite-volume, semi-Lagrangian
  - Double Fourier, spherical harmonics, spectral elements, discontinuous Galerkin (DG), and radial basis functions (RBF)

## Double Fourier series:

Strength: Exponential accuracy  
Computationally fast because of FFTs

Weakness: No practical option for local mesh refinement



## Spherical harmonics:

Strength: Exponential accuracy

Weakness: No practical option for local mesh refinement  
Relatively high computational cost  
Poor scalability on parallel computer architectures



## Spectral elements:

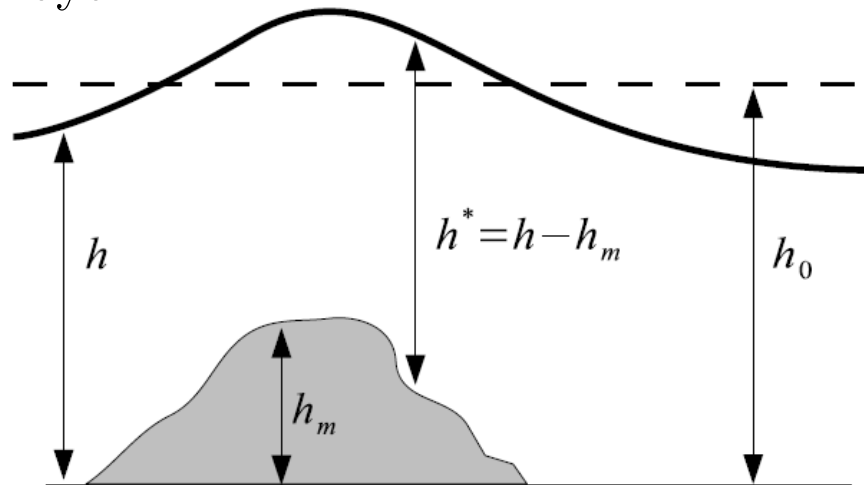
Strength: Accuracy approaching exponential  
Local refinement is feasible but complex

Weakness: Loss of efficiency due to unphysical element boundaries  
(Runge phenomenon - oscillations near boundaries → restrictive time-step)  
High algorithmic complexity  
High pre-processing cost

# Shallow water wave equations on a rotating sphere

Geo Seminar,  
Oct. 21, 2013

- Model for the nonlinear dynamics of a shallow, hydrostatic, homogeneous, and inviscid fluid layer.



- Idealized test-bed for horizontal dynamics of all 3-D global climate models.
- Governing equations in **spherical coordinates**:

Momentum:  $\frac{\partial \mathbf{u}_s}{\partial t} + \mathbf{u}_s \cdot \nabla_s \mathbf{u}_s + f \hat{\mathbf{k}} \times \mathbf{u}_s + g \nabla_s h = 0 \quad (\mathbf{u}_s = (u_s, v_s))$

Transport:  $\frac{\partial h^*}{\partial t} + \nabla_s \cdot (h^* \mathbf{u}_s) = 0$

- Using spherical coordinates is problematic for computational purposes.

# What's the problem with spherical coordinates

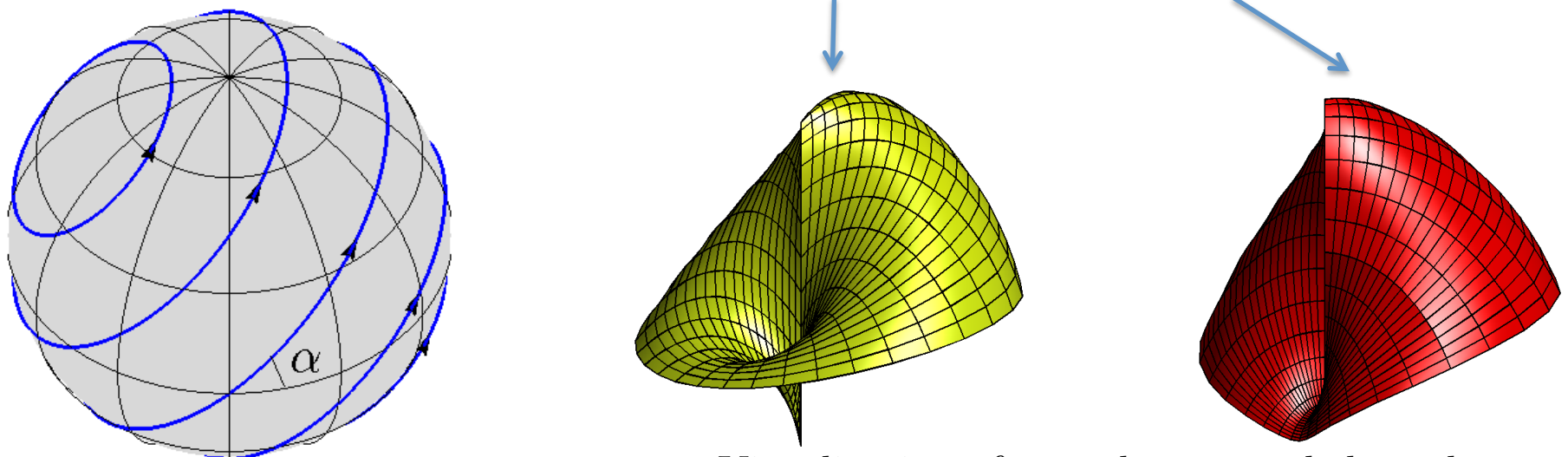
Geo Seminar,  
Oct. 21, 2013

- The pole problem!
- Differential operators (div, grad, curl) are singular at the poles:  
Latitude:  $-\pi/2 \leq \theta \leq \pi/2$    Longitude:  $-\pi < \lambda \leq \pi$

$$\nabla_s f = \frac{1}{r \cos \theta} \frac{\partial f}{\partial \lambda} \hat{\lambda} + \frac{1}{r} \frac{\partial f}{\partial \theta} \hat{\theta} \quad \nabla_s \cdot \mathbf{u}_s = \frac{1}{r \cos \theta} \left[ \frac{\partial u_s}{\partial \lambda} + \frac{\partial}{\partial \theta} (v_s \cos \theta) \right]$$

- Smooth vector fields can be discontinuous when expressed with respect to the spherical coordinate basis.

Ex: Solid body rotation  $\mathbf{u}_s = (\cos \alpha \cos \theta + \sin \alpha \cos \lambda \sin \theta, -\sin \alpha \sin \lambda)$



# (Surface) Div, Grad, Curl, and all that

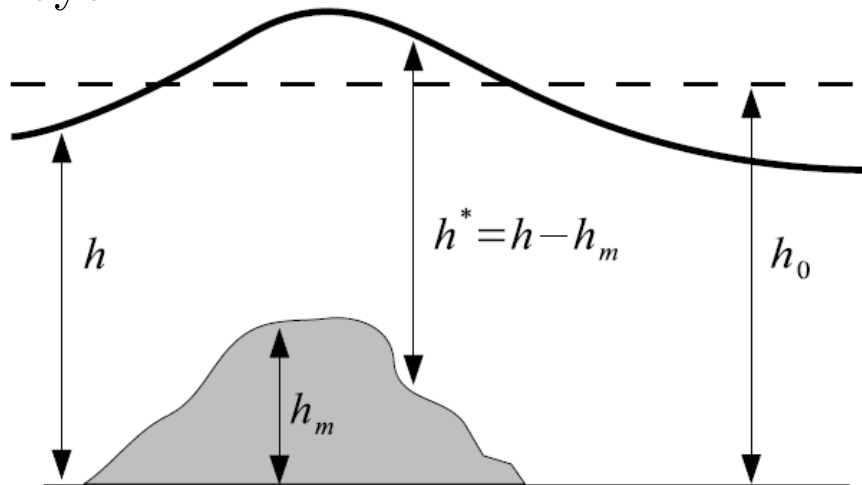
Geo Seminar,  
Oct. 21, 2013

Spherical Coords.	Cartesian Coords.
Point: $(\lambda, \theta, 1)$	$(x, y, z)$
Unit vectors: $\hat{\mathbf{i}} = \text{longitudinal}$ $\hat{\mathbf{j}} = \text{latitudinal}$ $\hat{\mathbf{k}} = \text{radial}$	$\hat{\mathbf{i}} = x\text{-direction}$ $\hat{\mathbf{j}} = y\text{-direction}$ $\hat{\mathbf{k}} = z\text{-direction}$
Unit tangent vectors: $\hat{\mathbf{i}}, \hat{\mathbf{j}}$	$\zeta = \frac{1}{\sqrt{1-z^2}} \begin{bmatrix} -y \\ x \\ 0 \end{bmatrix}, \mu = \frac{1}{\sqrt{1-z^2}} \begin{bmatrix} -zx \\ -zy \\ 1-z^2 \end{bmatrix}$
Unit normal vector: $\hat{\mathbf{k}}$	$\mathbf{x} = x\hat{\mathbf{i}} + y\hat{\mathbf{j}} + z\hat{\mathbf{k}}$
Gradient of scalar $g$ : $\mathbf{u}_s = \nabla_s g = \frac{1}{\cos \theta} \frac{\partial g}{\partial \lambda} \hat{\mathbf{i}} + \frac{\partial g}{\partial \theta} \hat{\mathbf{j}}$	$\mathbf{u}_c = P(\nabla_c g) = P \left( \frac{\partial g}{\partial x} \hat{\mathbf{i}} + \frac{\partial g}{\partial y} \hat{\mathbf{j}} + \frac{\partial g}{\partial z} \hat{\mathbf{k}} \right)$
Surface divergence of $\mathbf{u}$ : $\nabla_s \cdot \mathbf{u}_s = \frac{1}{\cos \theta} \frac{\partial u_s}{\partial \lambda} + \frac{\partial v_s}{\partial \theta}$	$(\nabla_c) \cdot \mathbf{u}_c = \nabla_c \cdot \mathbf{u}_c - \mathbf{x} \cdot \nabla(\mathbf{u}_c \cdot \mathbf{x})$
Curl of a scalar $f$ : $\mathbf{u}_s = \hat{\mathbf{k}} \times (\nabla_s f) = -\frac{\partial f}{\partial \theta} \hat{\mathbf{i}} + \frac{1}{\cos \theta} \frac{\partial f}{\partial \lambda} \hat{\mathbf{j}}$	$\mathbf{u}_c = \mathbf{x} \times (P \nabla_c f) = Q P(\nabla_c f) = Q(\nabla_c f)$
Surface curl of a vector $\mathbf{u}$ : $\hat{\mathbf{k}} \cdot (\nabla_s \times \mathbf{u}_s) = -\nabla_s \cdot (\hat{\mathbf{k}} \times \mathbf{u}_s)$	$\mathbf{x} \cdot ((P \nabla_c) \times \mathbf{u}_c) = -\nabla_c \cdot (Q \mathbf{u}_c)$
Here: $P = I - \mathbf{x}\mathbf{x}^T = \begin{bmatrix} 1-x^2 & -xy & -xz \\ -xy & 1-y^2 & -yz \\ -xz & -yz & 1-z^2 \end{bmatrix}$	$Q = \begin{bmatrix} 0 & -z & y \\ z & 0 & -x \\ -y & x & 0 \end{bmatrix}$

# Shallow water wave equations on a rotating sphere

Geo Seminar,  
Oct. 21, 2013

- Model for the nonlinear dynamics of a shallow, hydrostatic, homogeneous, and inviscid fluid layer.



- Idealized test-bed for horizontal dynamics of all 3-D global climate models.
- Governing equations in [Cartesian coordinates](#):

Momentum:  $\frac{\partial \mathbf{u}_c}{\partial t} + \mathbf{u}_c \cdot (P \nabla_c \mathbf{u}_c) + f \hat{\mathbf{k}} \times \mathbf{u}_c + g(P \nabla_c h) = 0$   $(\mathbf{u}_c = (u, v, w))$

Transport:  $\frac{\partial h^*}{\partial t} + (P \nabla_c) \cdot (h^* \mathbf{u}_c) = 0$

- Note that the flow is still constrained to surface of the sphere.

Governing equations:

$$\frac{\partial \mathbf{u}_c}{\partial t} = -P \begin{bmatrix} (\mathbf{u}_c \cdot P \nabla_c) u_c + f(\mathbf{x} \times \mathbf{u}_c) \cdot \hat{\mathbf{i}} + g(P \hat{\mathbf{i}} \cdot \nabla_c) h \\ (\mathbf{u}_c \cdot P \nabla_c) v_c + f(\mathbf{x} \times \mathbf{u}_c) \cdot \hat{\mathbf{j}} + g(P \hat{\mathbf{j}} \cdot \nabla_c) h \\ (\mathbf{u}_c \cdot P \nabla_c) w_c + f(\mathbf{x} \times \mathbf{u}_c) \cdot \hat{\mathbf{k}} + g(P \hat{\mathbf{k}} \cdot \nabla_c) h \end{bmatrix} \quad \frac{\partial h^*}{\partial t} = -(P \nabla_c) \cdot (h^* \mathbf{u}_c)$$

Overview of the procedure:

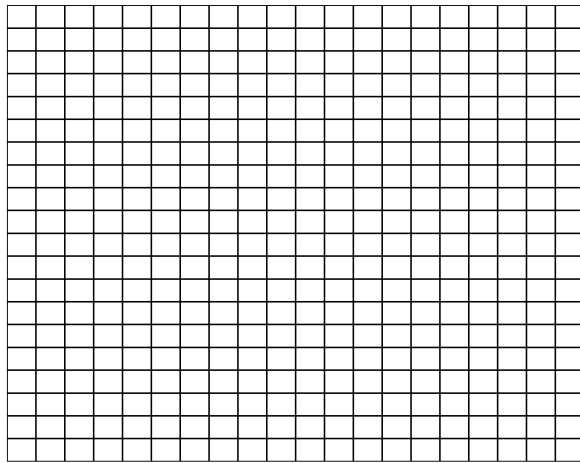
1. Choose some nice discretization of the sphere.



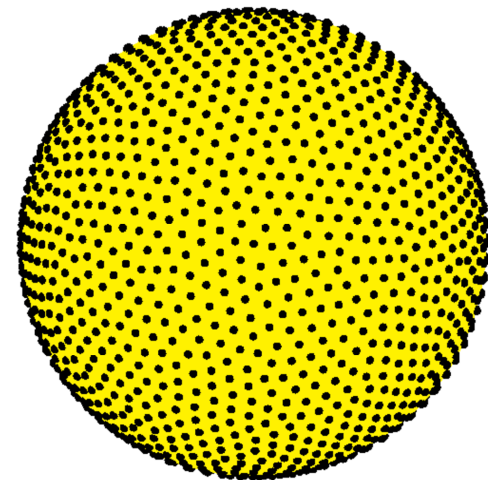
2. Replace unknowns with pointwise values at the discretization nodes.
3. Use finite-difference (FD) type formulas based on RBF interpolation for approximating the spatial derivatives in the governing equations at the discretization nodes.
4. Advance the system in time using some “standard” method for initial value problems (e.g. Runge-Kutta).

- Spatial discretization method: RBF-FD
- Generalization of standard FD formulas to “scattered” nodes:

Standard FD



RBF-FD



- 1. Require grids.
- 2. Derivative approximations are based on **polynomial approximations**.
- 3. Derivative approximations are local.
- References:
  - Wright & Fornberg (2006)
  - Fornberg & Lehto (2011)
  - Flyer, Lehto, Blaise, Wright & St-Cyr (2012)
  - Bollig, Flyer & Erlebacher (2012)

# Optimal nodes on the surface of the sphere

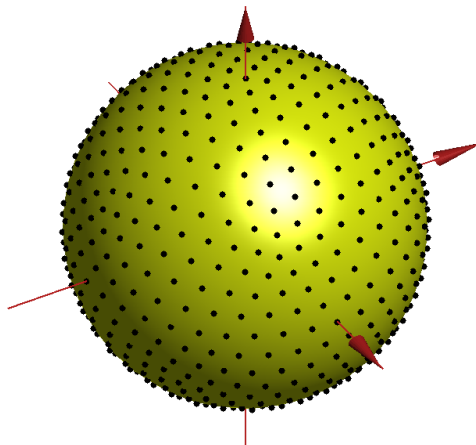
Geo Seminar,  
Oct. 21, 2013

- Some ideas for choosing a nice discretization of the sphere.

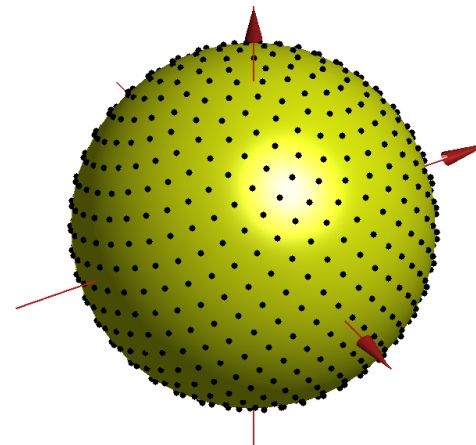
Examples:

Deterministic

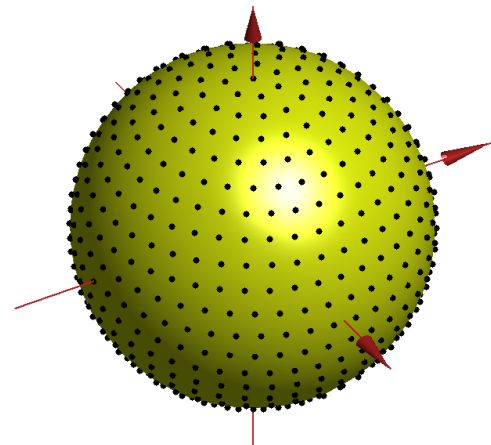
Icosahedral



Fibonacci



Equal area

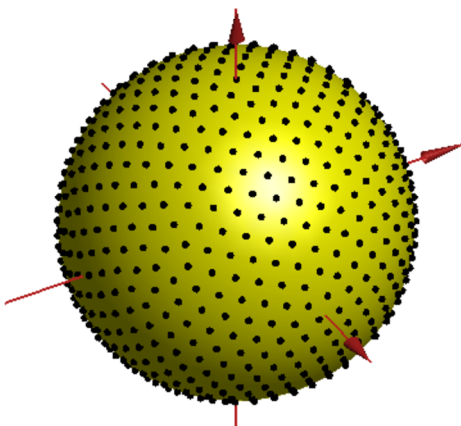


Swinbank & Purser (2006)

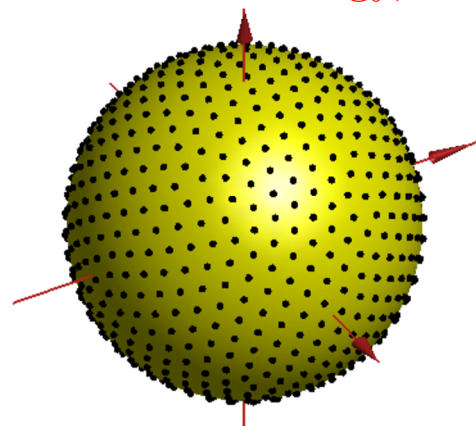
Saff & Kuijlaars (1997)

Non-deterministic

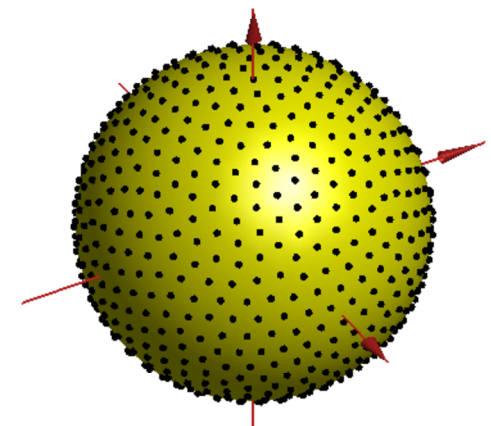
Minimum energy,  $s=2$



Minimum energy,  $s=3$



Maximal determinant

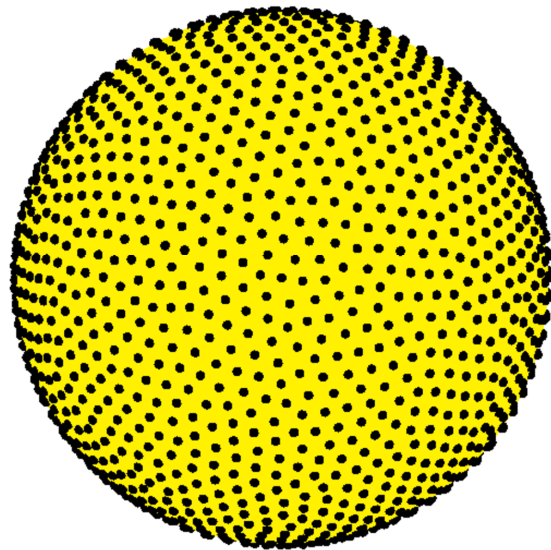


Hardin & Saff (2004)

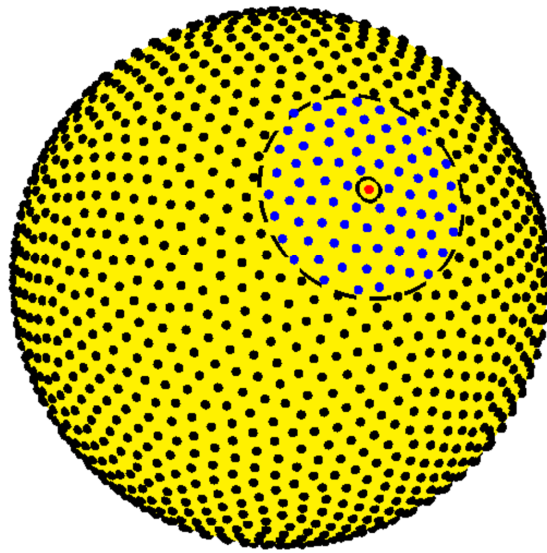
Riesz energy:  $\|\mathbf{x} - \mathbf{y}\|_2^{-s}$

Womersley & Sloan (2001)

- Start with some set of  $N$  nodes (on the sphere for current problem):



- Start with some set of  $N$  nodes (on the sphere for current problem):



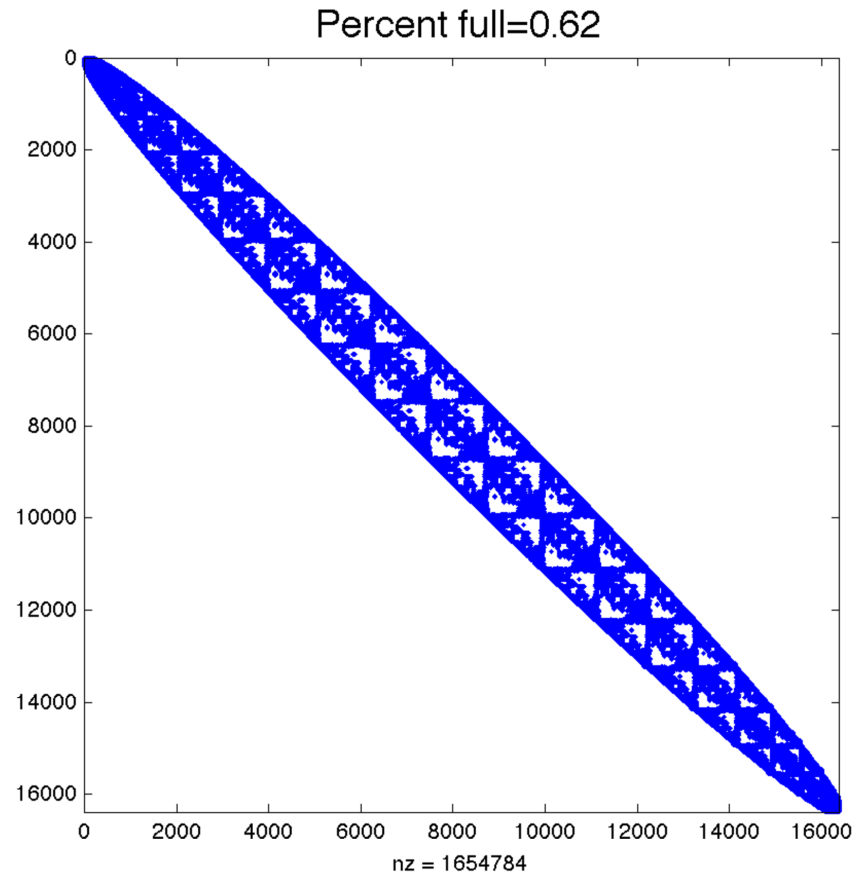
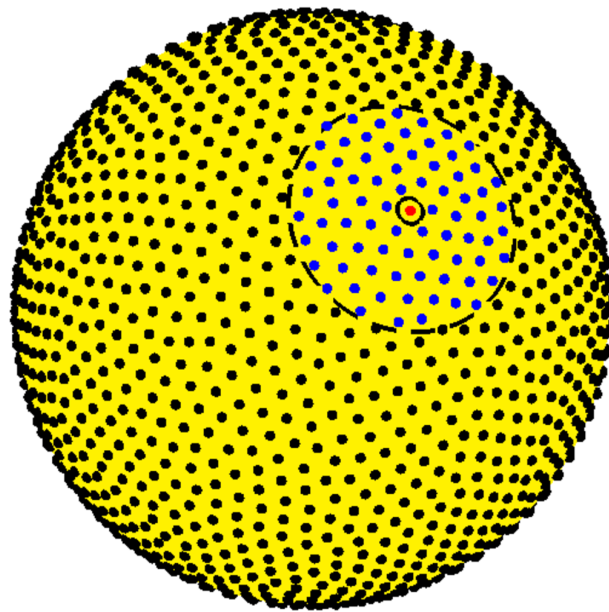
## Key Steps:

1. For each node  $\mathbf{x}_j$ , choose  $n - 1$  of it's nearest neighbors.
2. Construct RBF interpolant to the data over these  $n$  nodes.
3. Compute the derivative of the interpolant and evaluate at  $\mathbf{x}_j$ .
4. Use this to approximate the true derivative of the data.
5. Repeat for all  $N$  nodes.

# RBF generated finite differences

Geo Seminar,  
Oct. 21, 2013

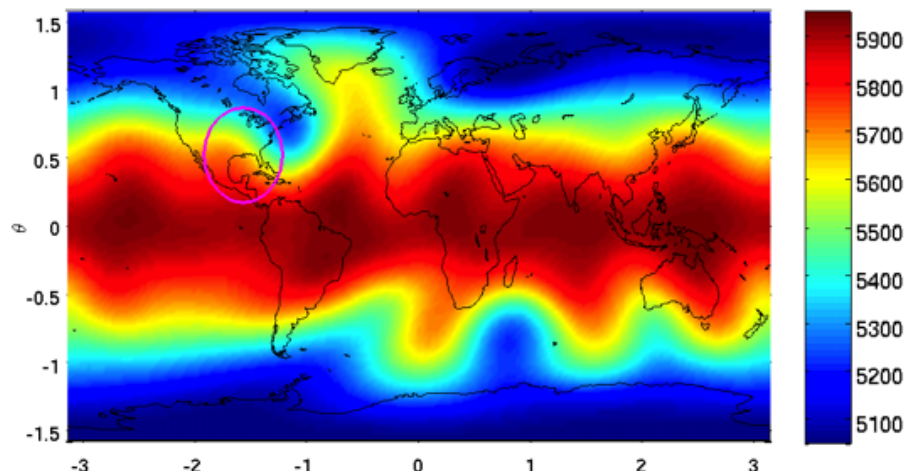
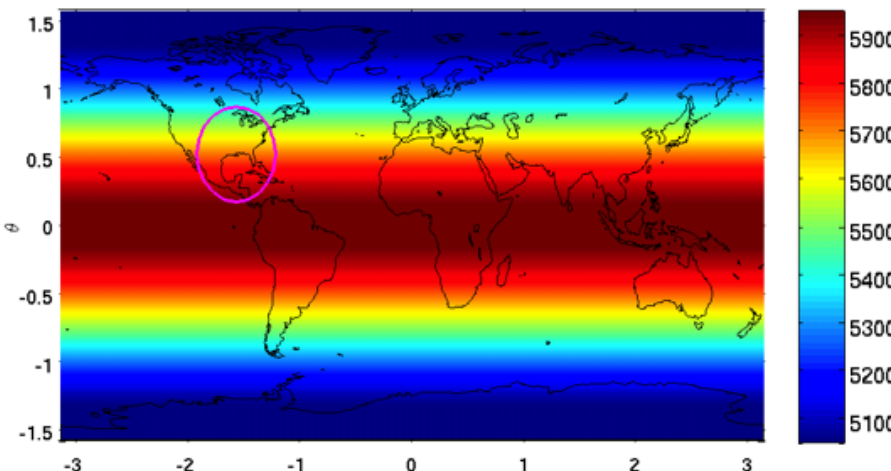
- The approximation can all be collected into one (sparse) matrix that operates on any function sampled on the nodes.
- Example differentiation matrix (DM) for  $N=16384$ ,  $n=101$ :



# Results from benchmark problem

- No analytical solutions are available for the shallow water equations on a sphere.
- Standard practice is thus to test new methods on accepted benchmark problems.
- We focus on the benchmark “Flow over an isolated mountain”:

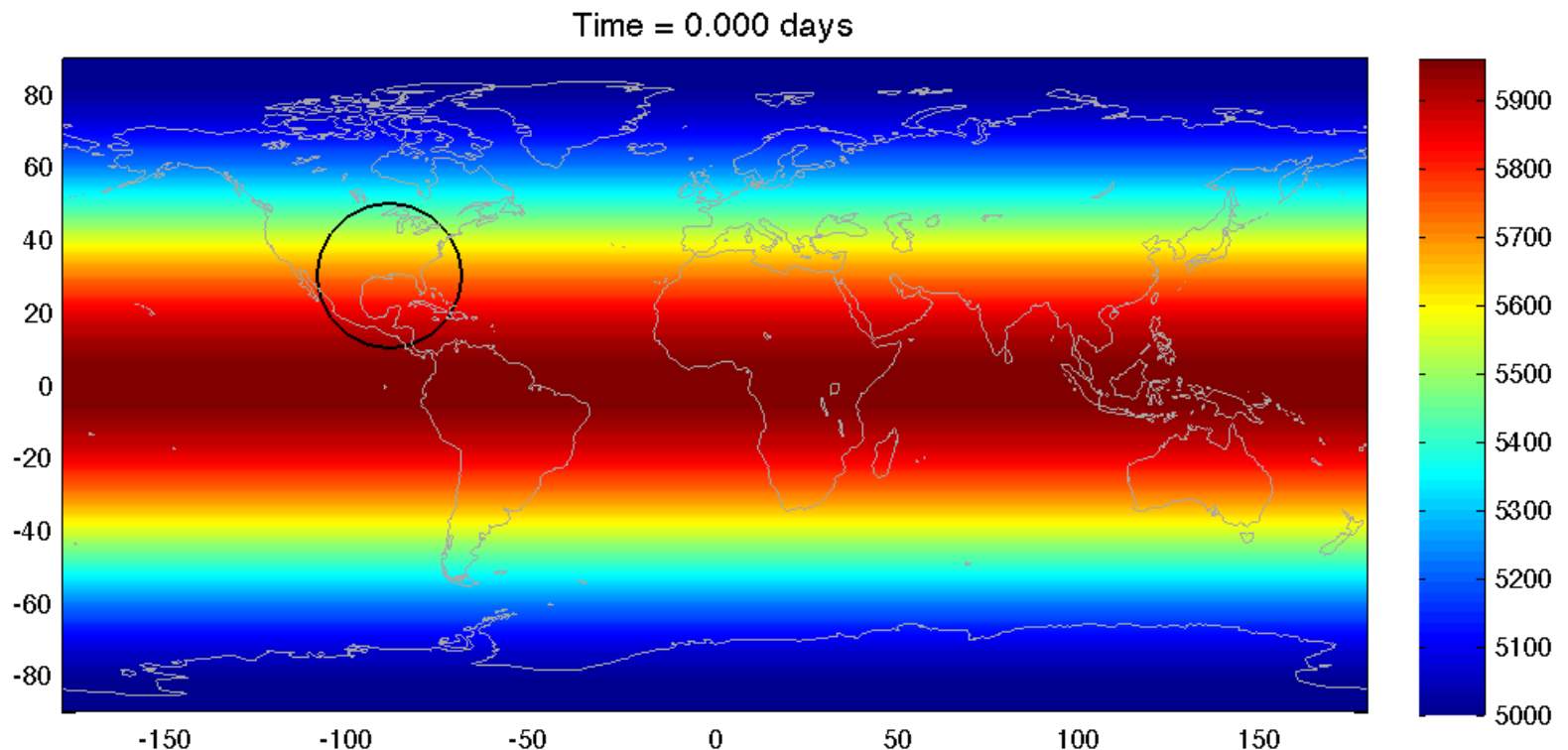
Height field at  $t=0$  days



# Flow over an isolated mountain:

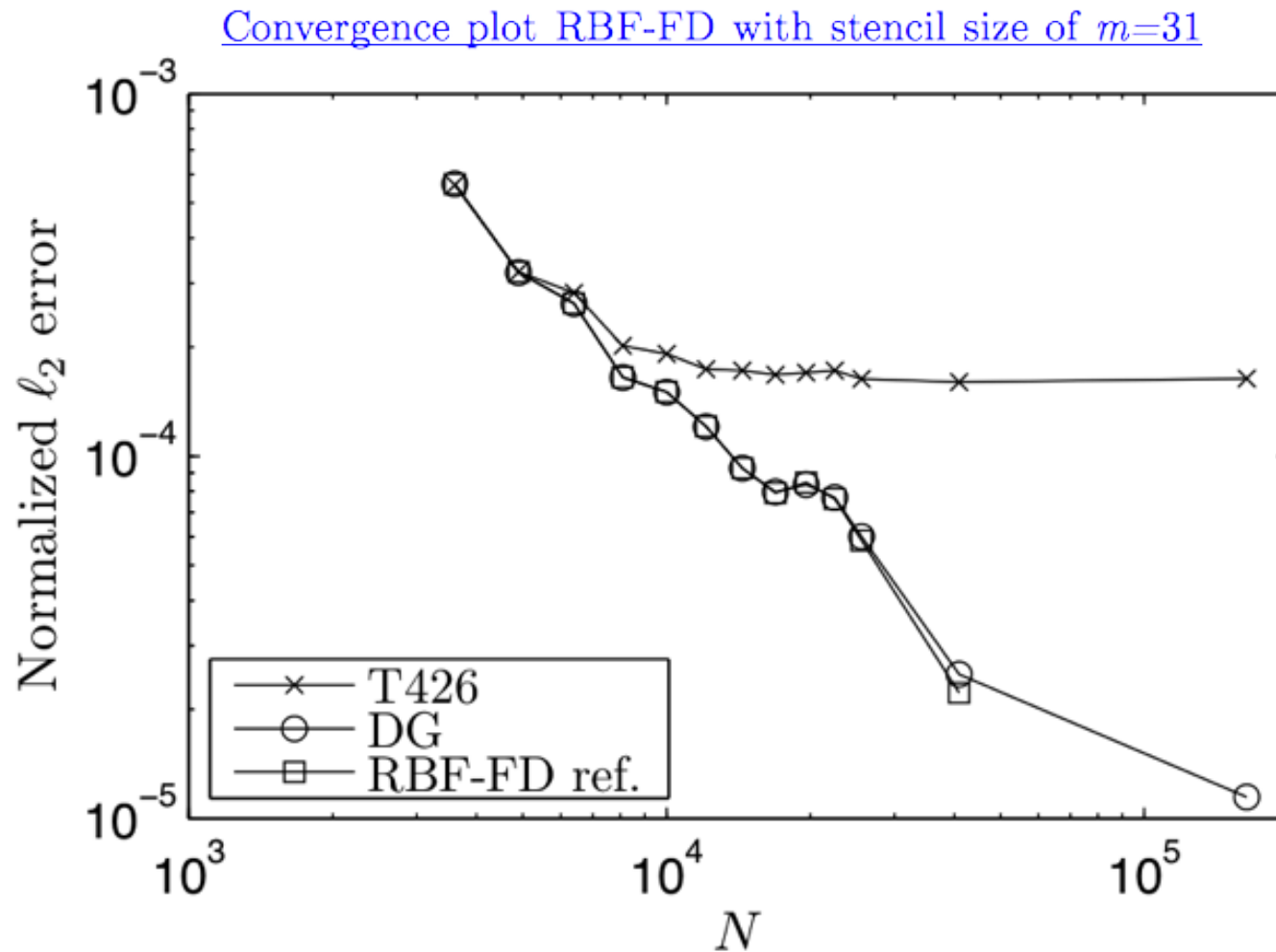
Geo Seminar,  
Oct. 21, 2013

- Visualization of the geopotential height field.



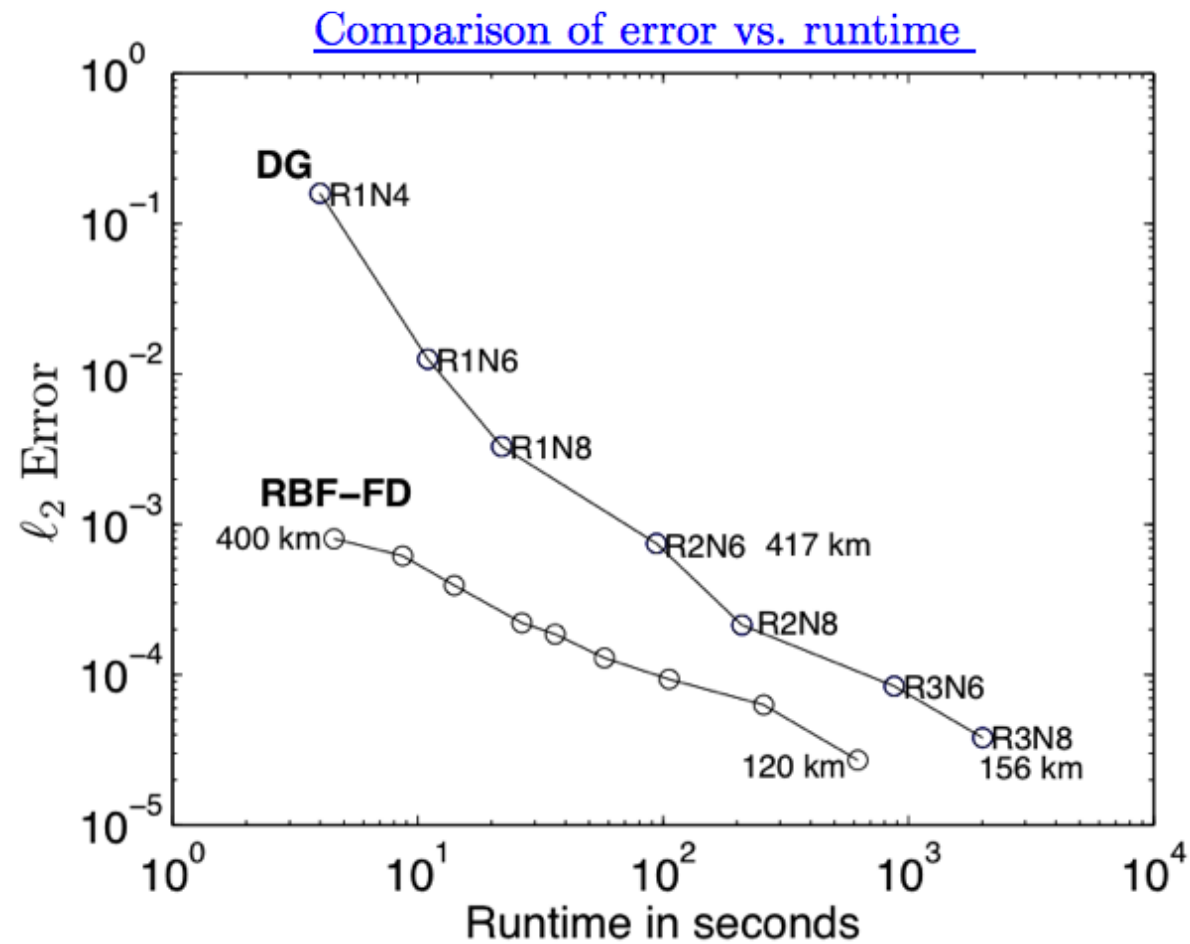
# Convergence comparison: 3 reference solutions

Geo Seminar,  
Oct. 21, 2013



- ✗ Standard Literature/Comparison: NCAR's Sph. Har. T426, Resolution  $\approx 30$  km at equator
- New Model at NCAR Discontinuous Galerkin – Spectral Element, Resolution  $\approx 30$  km
- RBF-FD model, Resolution  $\approx 60$  km

# Error vs. runtime comparison



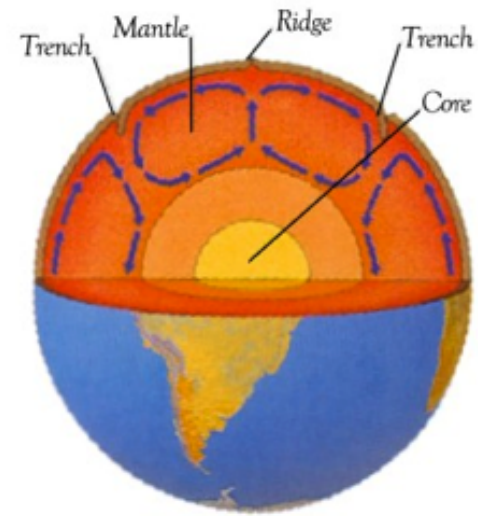
MacBook Pro, 2.2 GHz Intel i7 processor

- Further improvements for both methods may be possible using local mesh/node refinement near the mountain (actively being pursued).

# Mantle convection (isoviscous case)

- Model assumptions:

1. Fluid is incompressible
2. Viscosity of the fluid is constant
3. Boussinesq approximation
4. Infinite Prandtl number,  $\text{Pr} = \frac{\text{kinematic viscosity}}{\text{thermal diffusivity}} \rightarrow \infty$



- Non-dimensional Equations:

$$\nabla \cdot \mathbf{u} = 0 \quad (\text{continuity}),$$

$$\nabla^2 \mathbf{u} + \text{Ra} T \hat{\mathbf{r}} - \nabla p = 0 \quad (\text{momentum}),$$

$$\frac{\partial T}{\partial t} + \mathbf{u} \cdot \nabla T - \nabla^2 T = 0 \quad (\text{energy}).$$

- Boundary conditions:

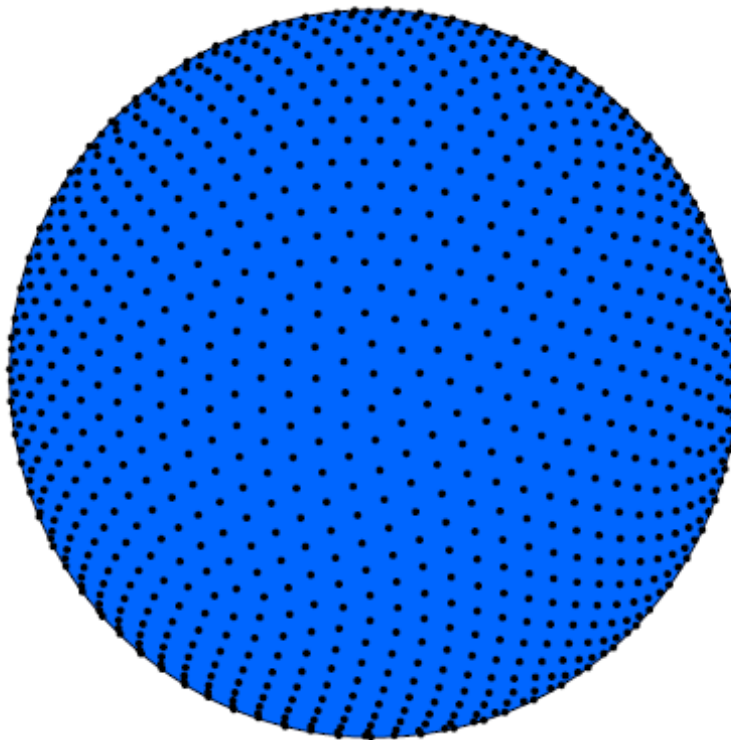
Velocity: impermeable and shear-stress free

Temperature (isothermal):  $T = 1$  at core mantle bndry.,  $T = 0$  at crust mantle bndry.

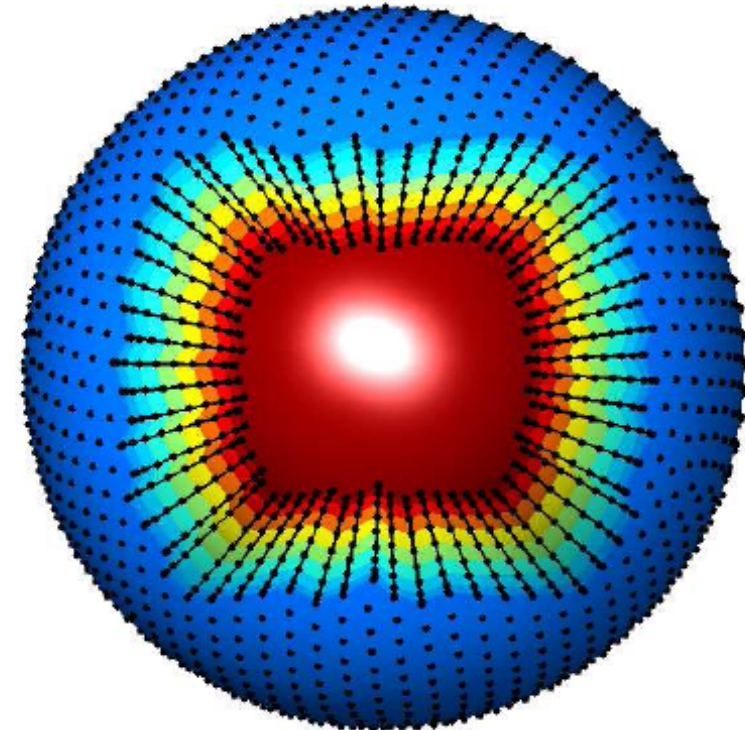
- Rayleigh, Ra, number governs the dynamics.
- Model for Rayleigh-Bénard convection

# Discretization of the equations

- Use a 1+2 hybrid approach  
 $M$  spherical surfaces with  $N$  nodes on each surface:



Use RBF-FD to approximate the horizontal components of the equations.



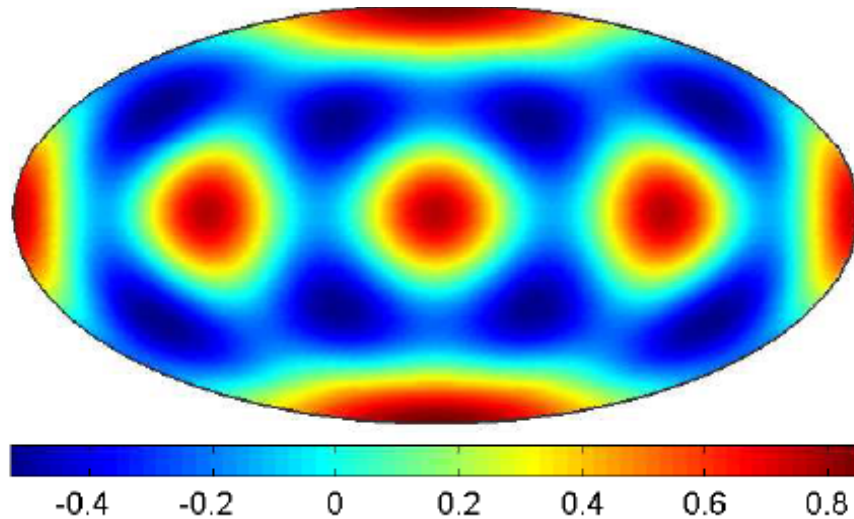
Use Chebyshev pseudospectral method for the radial components of the equations.

- Wright, Flyer, & Yuen (2010), *G-cubed*
- Flyer, Wright, & Fornberg (2014), Handbook of Geomathematics

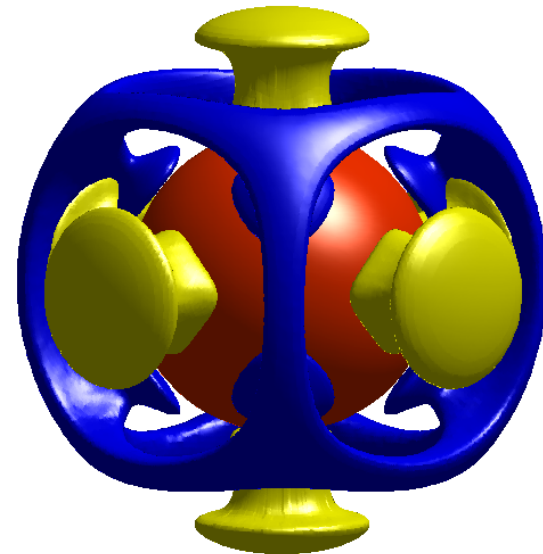
# Ra=7000 benchmark: validation of the method

Geo Seminar,  
Oct. 21, 2013

Perturbation initial condition:  $0.01 \left[ Y_4^0(\theta, \lambda) + \frac{5}{7} Y_4^4(\theta, \lambda) \right]$



Steady solution



Blue=downwelling, yellow=upwelling, red=core

- Comparison against main previous results in the literature:

Method	Nodes	Nu <sub>o</sub>	Nu <sub>i</sub>	$\langle V_{rms} \rangle$	$\langle T \rangle$
Finite elements (CitCom)	393,216	3.6254	3.6016	31.09	0.2176
Finite difference (Japan)	12,582,912	3.6083	—	31.0741	0.21639
Finite volume (FV)	663,552	3.5983	3.5984	31.0226	0.21594
Spherical harmonics-FD	552,960	3.6086	—	31.0765	0.21582
Spherical harmonics-FD	Extrapolated	3.6096	—	31.0821	0.21578
RBF-FD ( $n = 50$ )	59,823	3.6095	3.6096	31.0819	0.21577

## Model setup:

- Convective dominated flow
- $N=10,000$  RBF nodes ( $n=50$ ),  $M=81$  Chebyshev nodes
- Time-step  $O(10^{-7})$ , which is about 34,000 years
- Simulation time  $t=0$  to 0.1, which is just over 5 times the age of the earth

## Simulation:

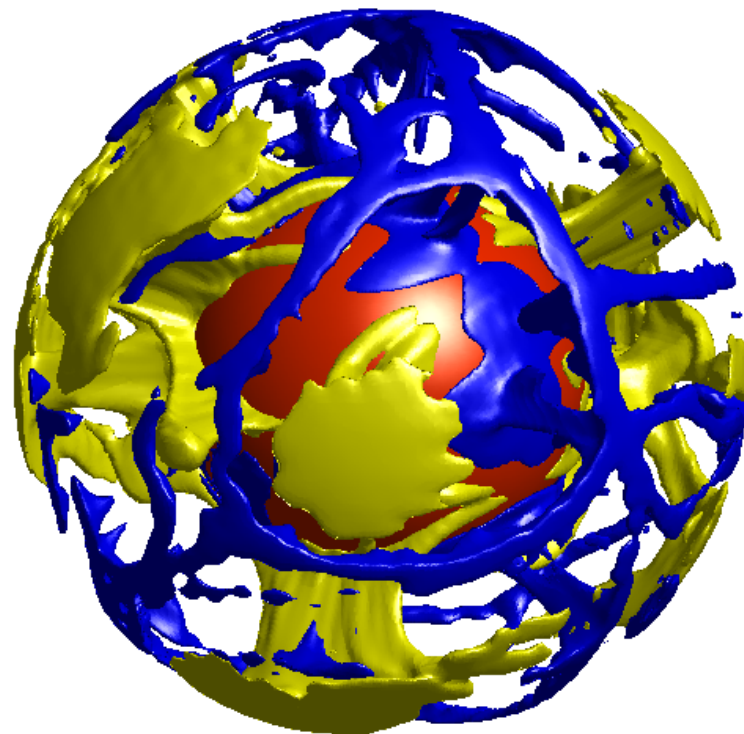
- Show isosurfaces of the residual temperature (difference from the mean).
- Blue=downwelling, yellow=upwelling, red=core

# Fully convective simulation: $\text{Ra}=10^6$

---

Geo Seminar,  
Oct. 21, 2013

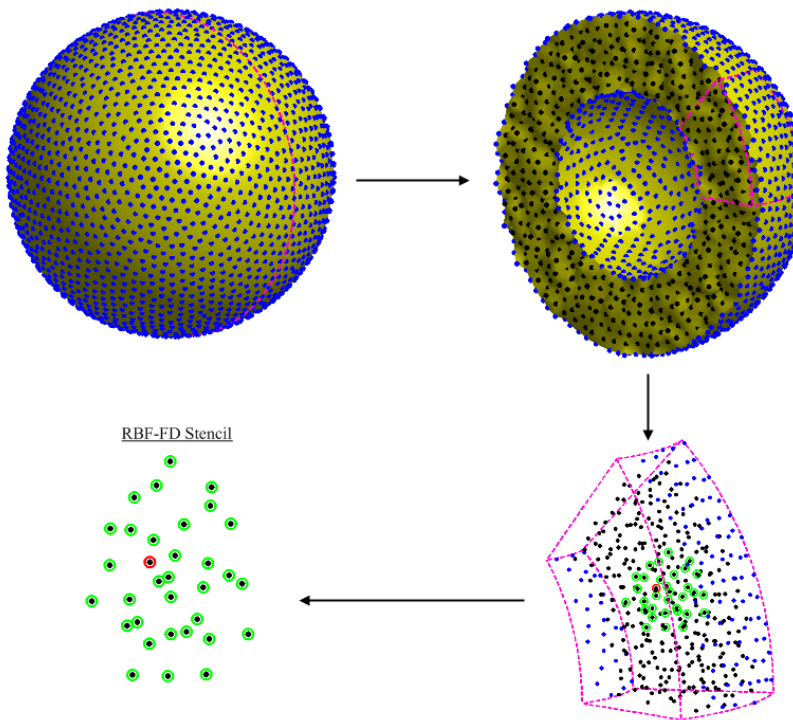
$t=0.00\text{e}+00$



# Current/future work for mantle convection

Geo Seminar,  
Oct. 21, 2013

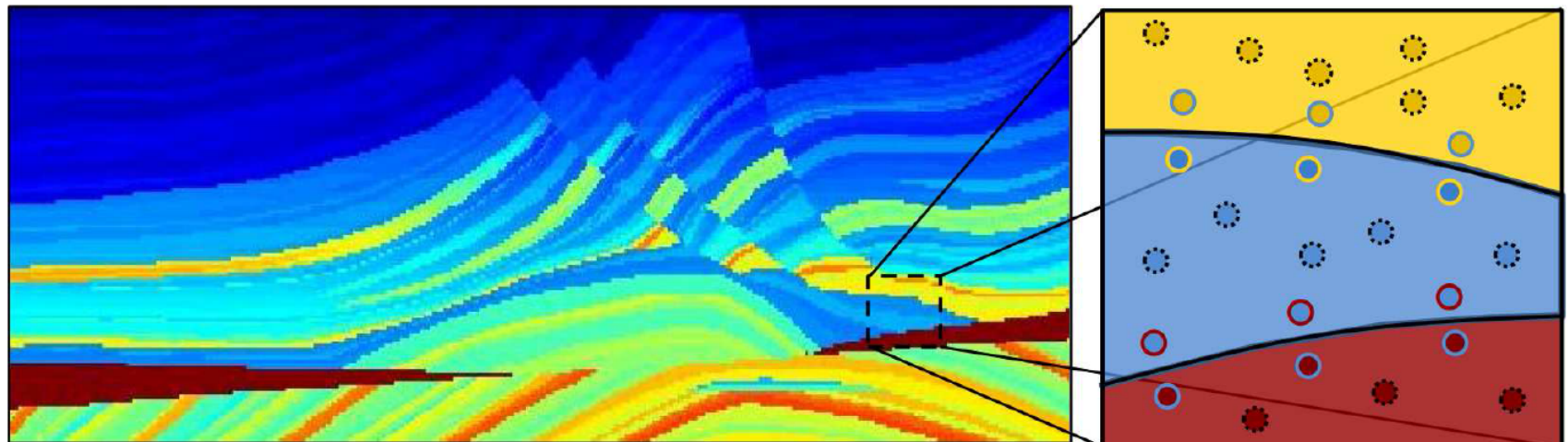
- Study sensitivity of the mantle convection model to initial conditions as well as computational model.
- Incorporate temperature dependent viscosity for more realistic model of the mantle.
- Go to full 3-D RBF-FD approximation (no hybrid approach):



# Future applications

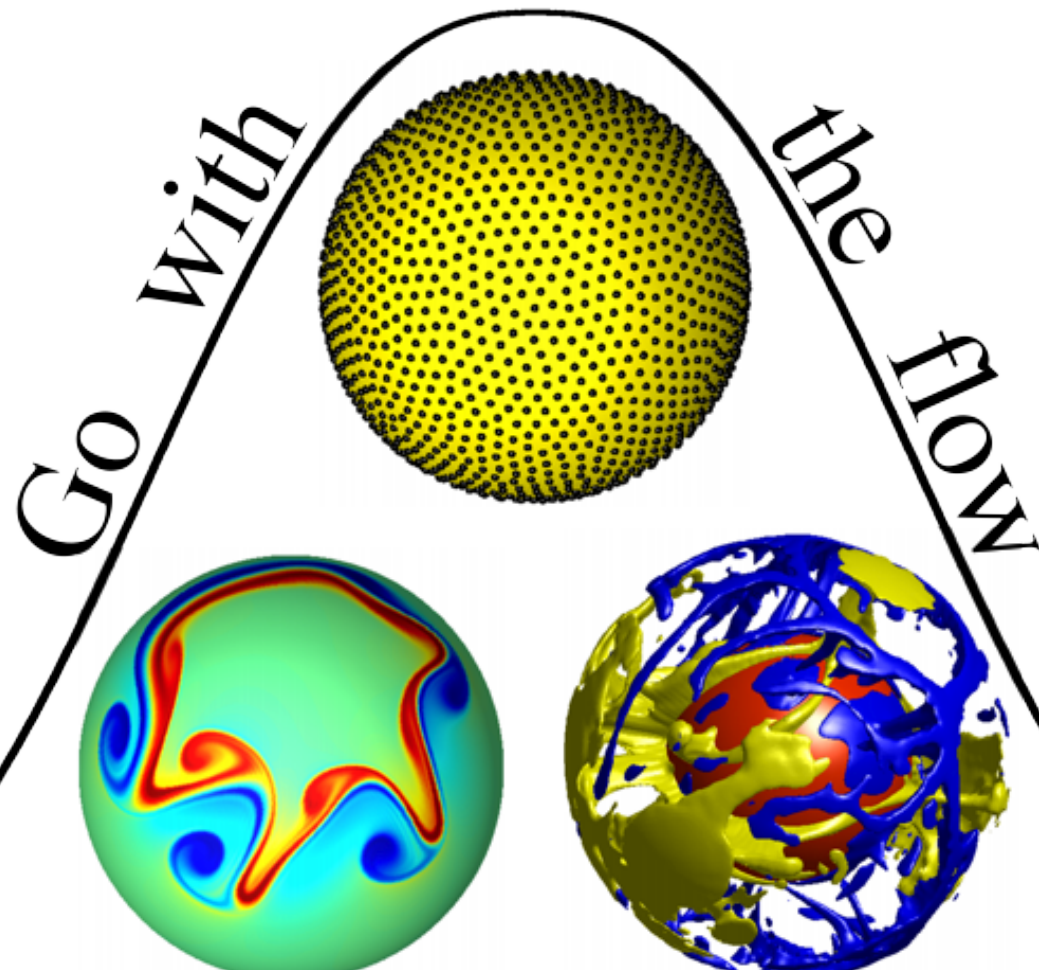
- RBF-FD for seismic modeling (2D elastic wave equation).

Seismic data for the Cuanza basin, Angola



Possible RBF-FD node layout for discretizing the equations across interfaces.

- N. Flyer (NCAR), B. Fornberg (Boulder), and A. St-Cyr (Shell).



Leave your mesh behind!